

Tidal Power Plant induced bed-scour assessment

*Morphological sea bed change modelling and
evaluation*



UNIVERSITY
.....
OF APPLIED SCIENCES

Tidal Power Plant induced bed-scour assessment

Morphological sea bed change modelling and evaluation

Author: Aleksas Vinskas (75900)

Course: Final Thesis (CU11020V12)

Education: Civil Engineering

Institution: HZ University of Applied Sciences

Study year: 2020-21, 2nd semester

In-company supervisor: Marco Gatto

Graduation lecturer: Sondos Saad Shaaban

Date of completion: 04 June 2021

Abstract

The research concerns a currently developed project of implementing a tidal power harnessing system in the structure of Brouwersdam. The system would exploit hydraulic head difference between two water bodies and using gravity caused flow, generate electricity. As a side-effect to such system, hydraulic activity would be created on either sides of the barrier, resulting in erosion of the sea bed.

The report aims to assess and estimate the change of bed morphology, magnitude and bed scouring in particular, if the intended tidal power plant was to be installed. The morphological change is decided by parameters of flow- flow velocity and its applied shear stress upon the bed particles and flow resistance capacity of the bed layer, determined by thresholds of critical velocity or shear stress at which bed grains are displaced.

A literature review is conducted to analyze and lay out the expected flow conditions at the location, modus operandi of sediment transport and bed scour phenomenon, hydraulic structures and bed protection presence influence for the development of scour. In addition, an algorithm to evaluate the relevant flow and sea bed properties and calculate bed scour is developed and provided in a concise scheme.

To evaluate the potential hydraulic conditions and bed scour severity around Brouwersdam, the developed scheme is applied using a time-dependent MATLAB model, leading to varying flow conditions and a slow and unsteady scour development process.

The results of the research display the effect the predefined boundary conditions have on the electricity production, magnitude of flow velocity and bed shear stress, and the critical particle flow resistance thresholds. All of which lead to the evaluation of scour development over time, its maximum depth and the span of the affected bed area.

Graphs and plots visualizing the investigated parameters over time and performed calculations lead to conclusions that more electricity could be harnessed if the boundary conditions were changed and that scour hole development will be rapid at its initial phase and decrease in development over time.

Preface

The document consists of a research report as central work for the graduation thesis at the HZ University of Applied Science. It is a part of a larger project called “Playing with Currents” concerning the Climate Power Plant tidal energy system. Carried out in the second semester of study year 2020-21, the research received a guiding stimulus and insight from various field experts.

Appreciation and thanks is sent towards lecturers M. Gatto and S. Saad for wise insights and a friendly guidance throughout the process and prior to it, during the previous study years. Also for J. Maas and B. Romboud from Delta Power research group for the financial aid and sparked inspiration for the value of the grand project. Additional gratitude is expressed for those mentioned for fostering growth and interest in the profession of a civil engineer.

It is hoped that the completed research lives up to the expectations and provides valuable findings and insight for further development and success of the Climate Power Plant.

Aleksas Vinskas

Leer, 04 June 2021

Table of Contents

1. Introduction	7
1.1. Climate Power Plant	8
1.2. Research description	9
1.3. Boundary Conditions.....	10
2. Theoretical Framework	9
2.1. Sediment transport	11
2.2. Flow properties and irregularities	12
2.3. Bed scour	14
2.4. Bed scour around hydraulic walls	16
2.5. Sea bed properties and flow resistance	18
2.6. Bed protection	19
2.7. Water hammer effect	20
3. Methodology	22
3.1. Data collection and modelling	22
3.2. What magnitude and scope of velocities will be generated?	22
3.3. Velocity at the bed layer	25
3.4. What magnitude of shear stress will be exerted on the sea bed?	26
3.5. What is the response of the soil located downstream of the power plant to external forces?	28
3.6. Equilibrium scour depth assessment	31
3.7. Calculation process scheme	34
4. Results.....	35
4.1. Varying water levels and valve positions.....	35
4.2. Duct outflow velocity magnitudes	37
4.3. Bed shear stress.....	40
4.4. Bed sediment response and deposition.....	42
4.5. Scour development and equilibrium depth.....	43
5. Discussion.....	47
6. Conclusions and recommendations	50
7. References.....	52
Appendix	55

Table of figures

Figure 1. Share of energy from renewable sources, 2019. Eurostat.	8
Figure 2. Grevelingen water level restrictions. Taken from "Climate Power Plant for Water Safety and Renewable Energy." by Prof. dr. ir. J. van Berkel, Ir. J.H. Maas, Ir. S.J. van Schaick and Ir. A. Heutink.....	10
Figure 3. Water levels in the North Sea and Grevelingen relation to electricity generation. Adapted from "Playing With Currents" by Ir. J.H. Maas, Ir. S.J. van Schaick, and Dr. ir. J. van Berkel.	12
Figure 4. Three-dimensional flow erosion visualization. Adapted from "Suppression of vertical flow separation over steep slopes in open channels by horizontal flow contraction. Y. B. Broekema ¹ , R. J. Labeur ¹ and W. S. J. Uijtewaal.	13
Figure 5. Bed scour shapes at different proximities between propeller and the wall and unconfined situation. Taken from "Propeller wash scour near quay walls" by G. A. Hamill, H. T. Johnston, and D. P. Stewart.	17
Figure 6. Conceptual Brouwersdam bed protection design. By M.H. Saase adapted from "The Conceptual Design of a Tidal Power Plant in the Brouwersdam"	19
Figure 7. Orifice flow between two basins. Retrieved from "Flow through lateral circular orifice under free and submerged flow conditions" by A. Hussaina, Z. Ahmadb, C.S.P. Ojha.....	23
Figure 8. Efflux velocity distribution. By M. H. van Saase, adapted from "The conceptual design of a Tidal Power Plant in the Brouwersdam".	25
Figure 9. Bed material types and their characteristic roughness coefficients. Retrieved from "Guide for selecting Manning's roughness coefficients for natural channel and flood plains"	28
Figure 10. Shields parameter and particle Reynolds number relation graph. Retrieved from "Introduction to Bed, bank and shore protection" (p. 64) by G. J. Schiereck and H. J. Verhagen.	29
Figure 11. Particles motion determination graph. Retrieved from "Simple general formulae for sand transport in rivers, estuaries and coastal waters" by L.C. van Rijn.	30
Figure 12. Bed protection conditions according to the value of Shields parameter. Retrieved from "Uncertainties in the design of bed protections near quay walls" by A. Roubos and H. J. Verhagen.	31
Figure 13. Bed protection length and factor a relation. Taken from "Introduction to bed, bank and shore protection" (p. 108) by G. J. Schiereck and H. J. Verhagen.	32
Figure 14. Velocity amplification factor as a function of relative sill height, bed protection length and bed roughness. Taken from "Scour Manual" by M. van der Wal, G. van Driel and H. J. Verheij	33

Figure 15. Critical initial slopes of scour hole. Retrieved from "Scour Manual" by M. van der Wal, G. van Driel and H. J. Verheij.....	33
Figure 16. Water levels fluctuations April 2021	35
Figure 17. Water level fluctuations April 01-29 2021	35
Figure 18. Water level fluctuations April 01-02 2021	36
Figure 19. Flow monitoring valves position during April 01-02 2021. The colored area display when the valves are open and flow is enabled.	36
Figure 20. Open valve durations on different time periods	37
Figure 21. Velocity values occurring at the outflow of a duct.....	37
Figure 22. Hydraulic losses.....	38
Figure 23. Velocity magnitude at the bed layer.	39
Figure 24. Velocities occurring at the exit of the duct and at the sea bed after reattachment.	39
Figure 25. Shear stress exerted upon sea bed graph.	41
Figure 26. Occurring shear stress values for fine and medium sands during April 27-29th 2021.....	41
Figure 27. Scour development in relation to time.....	45

1. Introduction

The modern World- its regions and people, unique and distinct in their cultures and ways of living are all facing one issue common and relevant to all- the Global Warming. In 1992, the United Nations Conference on Environment and Development, known as the Earth Summit was held, where climate change was first introduced as a global challenge for all its residents. The global event, occurring and showing evidence through recorded global temperature rise, warming and acidifying oceans, shrinking and retreating ice sheets, sea level rise (Intergovernmental Panel on Climate Change, 2014). Human living ways and activities resulting in large carbon and other by-products emissions, which has a tendency of heat capturing, discovered in the 19th century (Fourier, 1824), is the one true cause of such a worrying change. In the mentioned Earth Summit, an agreement by 154 countries on a Climate Change Convention was made. The main objective of which is: "stabilization of greenhouse gas concentrations in the atmosphere at a level that would prevent dangerous anthropogenic human-induced interference with the climate system. Such a level should be achieved within a time-frame sufficient to allow ecosystems to adapt naturally to climate change, to ensure that food production is not threatened and to enable economic development to proceed in a sustainable manner." (United Nations, 1992). By this way, states of the world had agreed to unitedly tackle the climate change by steadily reducing greenhouse gas emissions and changing the whole paradigm of the World economy.

Transferring onto the present day, when the international treaty on climate change evolved into Kyoto Protocol and Paris Agreement, setting to limit the global warming by 2 °C, the World has not been productive and proactive in regards to reducing emissions and shifting towards more sustainable ways of producing. Hence, the EU has come up with its own plan-the European Green Deal: to become the first climate-neutral continent by the year of 2050, decoupling economic growth from resource deprivation and including every person to take part. By that, all nations within the union ought to set plans to steadily reduce their greenhouse emissions to 0 for all its sectors, including the "hard-to-abate" (cement, steel, plastics, aviation, shipping, and heavy road transport) sectors as well. Change is inevitable for the energy sector as well, which is aware of clear pathways to shifting from fossil fuel to renewable energy and vast amount of development potential yet to be unlocked. Various renewable energy sources and means such as solar, wind and biomass energy are already exploited, the EU is steadily moving towards cutting out fossil fuel (figure 1), even if greater efforts were appreciated.

In the face of such a problematic situation, requiring very specific solving measures, development opportunities ought to be realized to have the most beneficiary effect. To make the energy transition towards renewables, which heavily depend on the local natural conditions of the area- such as geographical location, terrain properties, available natural resources, it is essential to recognize which sources could be the most effectively utilized, generating the best available energy returns. In the Netherlands, were renewable energy amounted only to 8.6% of the total energy consumptions in 2019 (CBS, 2020) new ways of renewable energy sources are vitally needed to be employed.

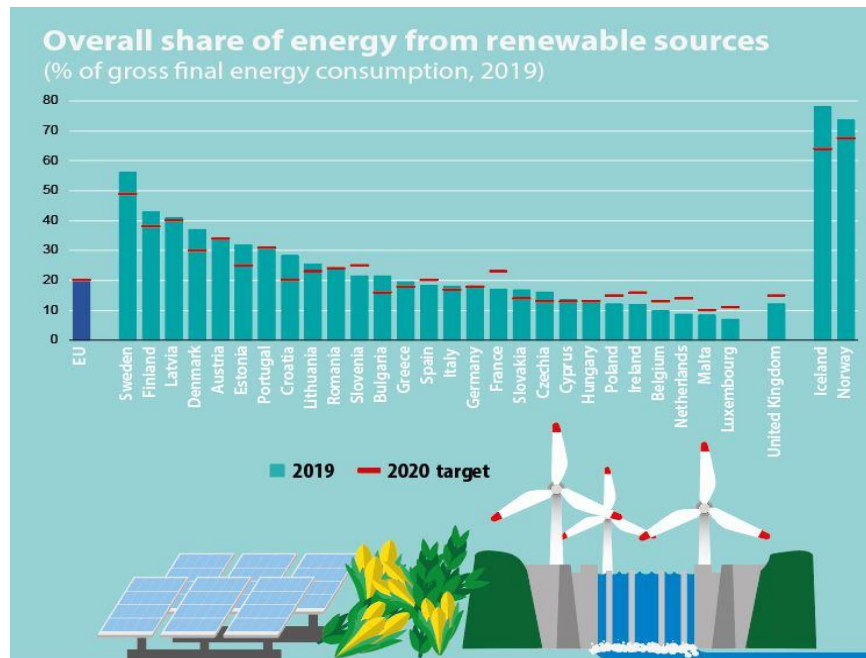


Figure 1. Share of energy from renewable sources, 2019. Eurostat.

1.1. Climate Power Plant

The Netherlands- a country having long and rich history has always had ties and relations to water- whether it was dominating the maritime and world trade or fighting tides and waves protecting its land from flooding. In result of which at present day the whole coastline of Netherlands is reinforced with dykes, dams and barriers from extreme storm events and is being extended seaward direction by nourishment works- Sand Engine being the biggest current undergoing project, expected to result in the widening of the beach along a 10 to 20 km stretch of the coastline and a beach area gain of 200 ha over a 20-year period (Marcel et al., 2013). In addition, several water bodies are closed off by barriers and dams, calming the inner conditions and allowing space for land reclamation for other purposes. Such dams are ideal to explore tidal power plants, harnessing tide energy as an additional renewable source. Currently, in several locations tidal energy is already harnessed: in Afsluitdijk and Easterscheldt Storm Surge Barrier. Ever since 1990 such plans are explored for Brouwersdam, which would also improve the water quality and the ecosystem of the closed-off lake Grevelingen (van Berkel et al., 2019).

The project initiated by Pro Tide, an organization working with tidal energy harnessing, is exploring implementation of a tidal barrage system in the mentioned Brouwersdam. A method of capturing large quantities of water flowing into a tidal basin and releasing it once the tide ebbs, through power generating turbines (Evans, 2007). A researchers' group under name of "Delta Power" has developed a project within the HZ University, supported by RAAK PRO program which funds researchers enhancing quality and capacity of applied research in the Netherlands. The fundamental idea proposed by Delta Power is to combine pumping stations and tidal power plants into one system, a so-called Climate Power Plant.

At the moment, investigations and research is performed exploring a flexible way of operating such system through use of a fast-switching device. According to the authors (Maas et al., 2018), to balance the portfolio of an electricity supplier and to prevent congestion in the electricity grid of the network operator at the same time and to enable the plant turbines to switch between pumping, holding and pumping modes within 10 s. Such a complex system, altering the structure of the Brouwersdam by being integrated within its walls, would change the hydraulic conditions within its premises by allowing a water flow to-and-from Grevelingen and the North Sea. Creating shear stress and velocity on the sea bed, it would result in the change of morphology due to induced scouring which will be the focal point of this research.

1.2. Research description

Problem statement:

As described before, investigations to implement a tidal power plant in Brouwersdam are ongoing. Installing tidal barrage principle based ducts for water flow and a Louvre valve inside of it to flexibly control pumping, holding and releasing discharge for electricity generation. Enabled flow is likely to cause bed scour around the premises of the barrier, requiring evaluation and assessment, as such a wash-out at the toe of the dam may lead to structure's equilibrium disruption and deformation progressively undermining the structure's foundation (Movahedi et al., 2018). Water flow moving to and from Grevelingen ought to be modelled and forecasted, to learn about the occurring velocities, shear stresses and a resulting the scour behavior and how severely it would affect the water bed.

Research goal:

To study bed scour occurring around the Brouwersdam structure premises due to a tidal power plant implementation - behavior and magnitude assessment.

Main research question:

What morphological change would be created on the bed of the North Sea and Grevelingen lake if a tidal power plant was implemented within the structure of Brouwersdam?

Sub-questions:

- What magnitude of velocities will be generated?
- What magnitude of shear stress will be exerted on the sea bed?
- What is the response of the soil located downstream of the power plant to external forces?

Purpose of the research:

The main aim of the research is to explore provide insight on the projected water flow navigating around the area of Brouwersdam and evaluate the characteristics of expected scouring while developing a scheme for its assessment. The research is carried out for the Delta Power research group of HZ University of Applied Sciences as a part of a larger project of Pro Tide project for the tidal power plant in Brouwersdam. The conducted research will assist in anticipating bed scour, designing the most optimal bed protection around the barrier and make further improvements for the grand project aiming to harness tidal energy and to contribute to the transition towards the climate neutrality.

1.3. Boundary Conditions

The founding base- a frame of requirements and a general assumptions have to be laid out within boundaries of which the research will be carried out.

The planned fast switching device monitoring the flow opens and shuts the valves under certain conditions. First and foremost, the system will be designed to operate within low-hydraulic head conditions not falling below 0.5m. The threshold above which energy production is possible (Berkel et al., 2018). Further on, as the flow would move in both directions during tidal floods and ebbs created by the pressure of water level difference between the two water bodies, the flow will occur on both sides of Brouwersdam. Along with it, bed erosion will take place too- on both sides. Therefore, flow and bed conditions need assessment in both directions.

To continue, certain water level height limits are defined for Grevelingen which need to be respected (figure 2):

WATER LEVEL RESTRICTIONS AT LAKE GREVELINGEN (RWS, 2018)

Upper limit	5 cm +NAP
Lower limit	45 cm -NAP
mean	20 cm -NAP

Figure 2. Grevelingen water level restrictions. Taken from "Climate Power Plant for Water Safety and Renewable Energy." by Prof. dr. ir. J. van Berkel, Ir. J.H. Maas, Ir. S.J. van Schaick and Ir. A. Heutink.

The water level restrictions were defined with respect to the water management system of the area, considering flood risks, transport infrastructure. Since it was defined by the Rijkswaterstaat, in charge of the inland waters and the road network, the investigation will be carried out within the bounds and will not be delved into furthermore.

Lastly, as the flow in a currently still water basin of Grevelingen will certainly lead to a change hydraulic conditions, bed scour is inevitable. For this reason, it is assumed that bed protection will be in place. Preliminary bed protection design was already performed by Saase (2018); hence the scour development will be explored downstream of it to find out the response of unprotected bed particles.

2. Theoretical Framework

To correctly and precisely evaluate the bed-scour projected to occur around Brouwersdam, natural processes and the inter-relations between one another ought to be analyzed, interpreted and understood. Numerous variables having effect to bed-scour magnitude and behavior are to be considered. The very process of calculation, projection and modelling of sediment transport is complex and difficult to be forecasted- the mentioned multitude of variables such as occurring flow velocities, forces, irregularity of soil property, factor of “unknown unknowns” makes the science of sediment transport intricate and requiring deep comprehension. Nevertheless, more simplified methods can still provide valuable results and insight for further studies if correct assumptions and interpretations are made, after gathering the right input data and processing it with the right research methods.

2.1. Sediment transport

In its essence, sediment transport is a movement of suspended solids due to influence of flowing fluid and gravity. It can act by different mechanisms and in different mediums, the one important for this research case is wave and tide activity induced deposition. It is mostly responsible for shaping coastlines and beaches by either accreting or depositing sediment, which results from a sediment balance- either a deficit or a surplus. What matters in such type of sediment transport and coastline shaping, is whether the location is wave or tide dominated. According to Komar (1991), it reflects the relative sediment transport capacity of the tidal currents against the wave-generated long shore currents. Sediment moved by tidal currents accumulates in large back-barrier flood-tidal deltas where it is sheltered from wave dispersal (Moore et al., 1991). Given the situation of Brouwersdam and the planned Climate Power Plant, to be operating as a tidal barrage, the flow is allowed when there is a significant water table difference between the North Sea and Grevelingen. As displayed in figure 3, the ducts are open and flow is enabled- electricity is generated at a hydraulic head difference above 0.5m, when efficiency reaches 0 according to Berkel et al. (2018). As the flow is controlled by shut or open waves, it could not be said that that the system is tide dominated- the gravity and pressure difference are main determinants of the flow parameters, having influence on the mode of sediment movement as well.

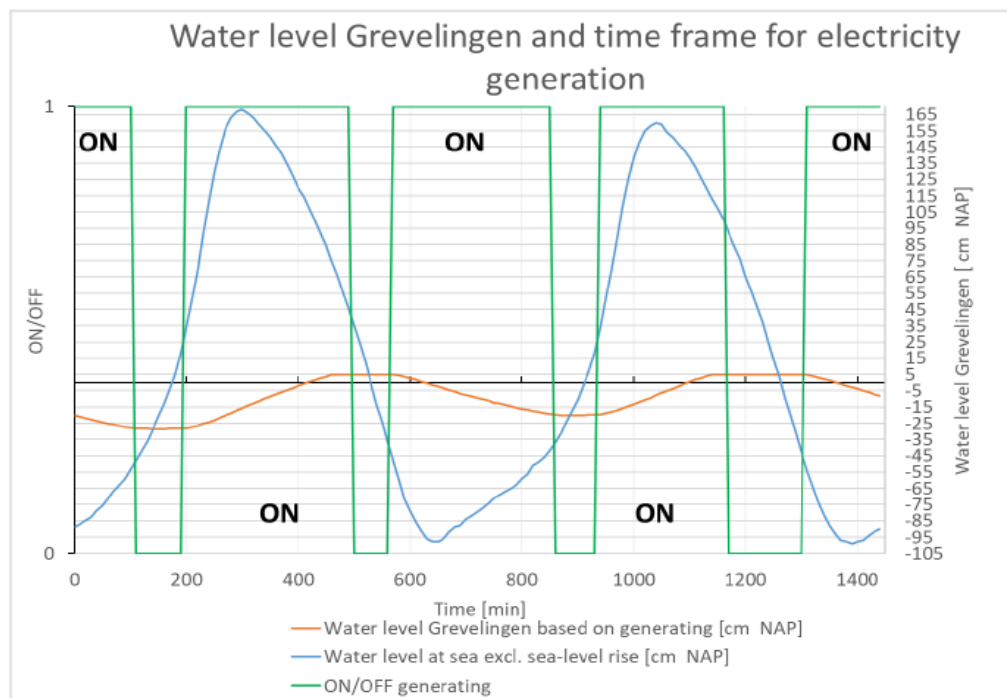


Figure 3. Water levels in the North Sea and Grevelingen relation to electricity generation. Adapted from "Playing With Currents" by Ir. J.H. Maas, Ir. S.J. van Schaick, and Dr. ir. J. van Berkel.

Sediment is entrained by the induced bed shear stress (Nielsen, 2015) generated by wave motion, indicating a relation between the magnitudes of flow velocity and bed shear stress, both covered in the research questions. Nevertheless, another important factor is the response of individual particles, decided by its physical parameters and properties and position within the bed layer- grains at the surface are much more vulnerable to deposition. For fine-grained, cohesive sediments the mobility may even depend on the history of consolidation and biological activity (Nielsen, 2015). Therefore, knowing that rate and behavior of suspended solids transport are determined by parameters of both- the flow and the sediment, it is needed to be obtained as an input data for bed scour evaluation.

2.2. Flow properties and irregularities

The planned hydraulic system- an array of ducts carrying flow controlled by a valve- will lead to complex flow conditions of a non-uniform flow involving flow separation and mixing, turbulence, and pressure differences vertically and horizontally (figure 4) due to how the system is arranged and how the expected bed scour would redirect the pressure gradient to act against the local flow direction according to Simpson (1989). Understanding how the flow behaves in the system is paramount to predict the morphological change and design according bed protection.

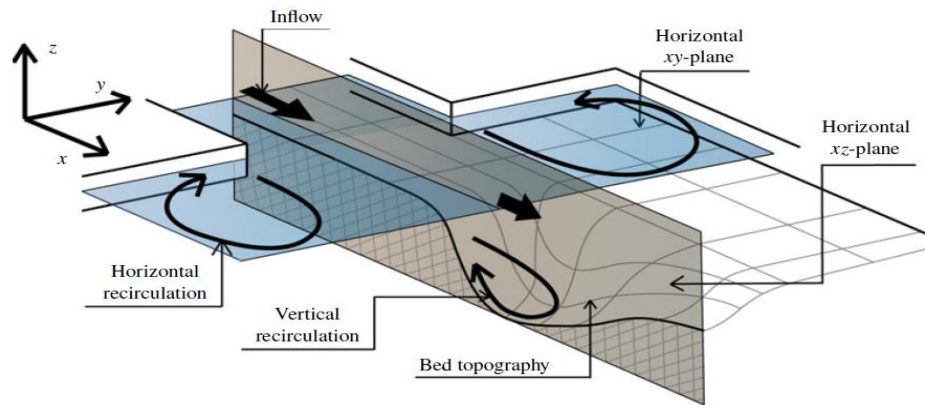


Figure 4. Three-dimensional flow erosion visualization. Adapted from "Suppression of vertical flow separation over steep slopes in open channels by horizontal flow contraction. Y. B. Broekema1, R. J. Labeur1 and W. S. J. Uijtewaal.

Reasons why a flow upstream the dam when it enters the system being steady and uniform turns into a turbulent and irregular eddy flow are several- geometrical and hydraulic. It must be noted that flow turbulence is influenced by acceleration or deceleration of the flow (Schierreck & Verhagen, 2012) which is exactly what can be expected in the Climate Power Plant situation. As known from the volumetric flow equation, discharge of the flow is directly tied to the velocity and the cross-sectional area of the flow (Engineers Edge):

$$Q = v * A$$

The water flow entering the duct would suffer from contraction of the flow field limited by the duct's geometry and accelerate as a result of Bernoulli's law of energy conservation (Batchelor, 1967). Once the water exits the duct entering the basin of Grevelingen, it is freed from geometrical constrictions, suddenly expands vertically and horizontally and decelerates.

Exiting out of the duct triggers more factors enhancing turbulence and eddy flow. A mixing layer is starting to form as a result of velocity differences. The mean outflow velocity is highest in the center decreasing towards the sides (Broekema et al., 2018). Each duct, within a system, is separated by a partition according to the conceptual design by Saase (2018). At these partitions velocity should be minimal while along the whole array of ducts the velocity would differ significantly- causing a mixing layer. The stagnant fluid will accelerate, whereas the flowing mass will lose momentum. In the mixing layer the shear stress is intense, inducing turbulence (Schierreck & Verhagen, 2012). Figure 4 displays that flow mixing occurs in horizontal and vertical planes. This influences development of the boundary layer- a flow region in the vicinity of a surface- the bed. Mixing and decelerating flow thickens the boundary layer, leading to a flow separation due to the pressure gradient acting against the local flow direction (Broekema et al., 2019). The separated flow increases turbulence and the caused load (Schierreck & Verhagen, 2012). Such a mixing and recirculating state of flow occurs within a certain segment until the main flow reattaches to the bed and gradually regains uniform condition (Wal et al., 1991), growing a new boundary layer and obtaining an equilibrium state (Schierreck & Verhagen, 2012). According to the very same Schierreck and Verhagen (2012), the location of the

reattachment is the critical one for bed protection: the pressure there is higher than in the recirculating area where the water entrainment in the flow takes place. Broekema (2020) too implies that the bed shear stress peaks at the reattachment point. Suggesting it cannot be overlooked when assessing bed protection. Nevertheless, the mixing zone is the primary target as it is closer to the dam which makes it more crucial regarding safety. Due to high turbulence energy (Hoffmans & Pilarczyk, 1995) and for other reasons explained further.

2.3. *Bed scour*

The natural phenomenon is a long-time known and a troubling issue for engineers. Local bed scour, tending to occur around bridge piers, at ports next to quay walls over time can lead to severe structural damage if no precaution or mitigation measures are taken. Being a particular type of sediment transport, bed scour acts by washing out sediment around hard structures. Magnitude and behavior of it depends on two groups of factors: nature of the flow occurring by the bed and properties of the particles exposed to it. To add, a third important variable in bed scour events is the hard-structure, in relation to which bed-scour takes place.

Arising from water activity around hydraulic structures, it has had attracted attention of researchers, trying to comprehend and searching for methods to precisely estimate it. Various methods have been invented to calculate it on different occasions (Bormann et al. (1991); Hoffmans & Booij (1994); Chatterjee et al. (1994); Hoffmans (1998); Rudolph et al. (2009), etc.). In one or another form they assess magnitude and behavior calculations or provide bed-scour characteristics. Yet few researches cover tidal-barrage induced bed scour in the premises of a dam. For this reason, comparable links ought to be drawn to researches exploring resembling but not exact settings. For example, investigations addressing propeller jet induced bed-scour nearby quay walls- a common issue for ports (Hamill et al., 1999). Fundamental ideas and universal scour characteristics are to be drawn and adapted to the case of Climate Power Plant in Brouwersdam.

Past studies prove that velocities and shear stresses are decisive in erosion rate (Crowley et al., 2020) and that velocity is responsible for the depth of the scour hole- the higher the velocity, the bigger the wash-out (Roubos & Verhagen, 2007), (Hoffmans, 1998). Yet the parameters mentioned, are resultants of vector forces acting in different directions and influencing the particles differently. To identify these velocities, measurement devices, such as acoustic Doppler velocimeter, are used to determine flow velocities acting axial radial and tangential directions (Chin et al., 2002). Hoffmans (1998), claims that the forces acting upon bed particles over which a fluid is flowing are the submerged weight of the particles, the lift forces, and the drag forces. All of these components should be within the field of attention when searching for scour alleviation measures.

The manner of sediment transportation-how the scour develops within the effect area is also worth attention. As described by Schiereck and Verhagen (2012) two types of scouring may occur, depending on flow and sediment conditions upstream:

- Clear-water scour- resulting from either lack of sediment transport capacity- the flow being too weak to bring in grains from upstream to replace the deposited ones in the scour hole which is a cause of change in the flow properties. Or it can be due to bed particles upstream being too rigid for suspension and resisting the erosive forces while downstream it may not, where it continues until an equilibrium depth is reached by velocity dropping below the critical threshold. In other more simple words, clear water scour occurs if the sediment transport from upstream is zero and positive in the scour hole (Hoffmans & Booij, 1993).
- Live bed scour, when the upstream flow transportation capacity suffices but due to the hydraulic structure caused accelerations and decelerations inducing turbulence and increasing the very same transportation capacity, the wash out worsens along with it. Such scour lasts until the erosion capacity in the hole is equal to the supplied sediment capacity from upstream.

There are slight differences between the two types but a condition of transport rate from the scour area being larger than that of the upstream is definitely common for both types. Concluding that negative or positive sediment deposition is the best distinguisher to know if scour takes place or not, works of Bormann et al. (1991); Hoffmans and Booij (1993); Hoffmans and Pilarczyk (1995); Schiereck and Verhagen (2012) indicate it.

How and where scour would take place depends on the resistance of the bed: particle diameter, the size distribution, the grain shape, the density of the sediment, the cohesion of material and the turbulence level near the bed (Hoffmans, 1998). Particles displacement also relies on the bed consolidation and composition of the soil. A well-compacted layer is more durable against scouring effect (Movahedi et al., 2018). Such resilience may be temperate as scouring is a dynamic process, meaning that magnitudes, frequencies and durations are ever-changing and ought to be considered in relation to time (Whittaker & Schleiss, 1984). All of these relevant agents prove that bed-scour is a complicated phenomenon to be adequately forecasted. Lateral non-uniformity of the flow, significantly adds to complexity of scour estimation, likely to impact the hydrodynamics in the scour holes vicinity (Labeur & Uijttewaal, 2019).

Concerning the scour development process- it is inevitable, whether growing nearby the dam or further away. The just explained scouring nature confirms it. As soon as an area is not sufficiently supplied with sediment from upstream scour will take place. Implemented bed protection must suffice to resist the subjected stress exiting the duct, denying sediment transport and material supplies to the area downstream suffering from eroding forces and losing soil. Moreover, the scour pit growth is self-inducing as research claims (Broekema, 2019); (Schiereck and Verhagen, 2012); (Broekema et al., 2018). The slope of the scour hole, which forms as the sediment is removed, amplifies flow separation and mixing discussed in the previous chapter. A separation leading to water flowing against the main flow direction as visible in figure 3, all within the scour hole- further entraining sediment and deepening it. As Schiereck and Verhagen (2012) put it: scour causes scour. Yet this process is not continuing forever: the larger the hole gets, the more energy and velocity is lost. Either the depth or the slope steepness will become such that the flow velocity will be smaller than the sediment entrainment threshold (Broekema, 2020). Then the scour hole reaches asymptotic state defined as the depth at which no appreciable further scour will

take place (Hamill et al., 1999). It can be considered as the equilibrium depth albeit the scour may still continue at insignificant rate (Bey et al., 2007).

For bed protection design and construction process reasons, scour hole depth and its development in time are the most interesting topics regarding this process. For the construction phase and maintenance policy the rate of development could be decisive, while scour depth may affect the choice of bed protection design (Schiereck & Verhagen, 2012). Since the explored situation is considered to not have a bed protection installed, the equilibrium scour depth should be of interest rather than its development in time. As Schiereck and Verhagen (2012) put it: scour without bed protection usually develops quickly, which makes sense given the porous and fine nature of sand.

2.4. Bed scour around hydraulic walls

Scouring tends to behave differently around different type structures. The situations of focus to comprehend behavior around Brouwersdam are those around quay walls and barriers, where it would create an obstacle for water flow and have a disposition area, for instance, downstream where sediment could be disposed. More importantly, response of the wall to scouring is as crucial, as it becomes the decisive element in shaping the scour hole and the morphology of the bed.

In situations of a propeller acting on a quay wall, the distance between the two becomes the main factor of what shape the scouring shall take: the proximity of the wall will cause a deflection of the propeller wash toward the bed, enhancing any scour that would have resulted had the quay not been present (Hamill et al., 1999). Comparing it to unconfined conditions where scour is not limited by wall presence, the behavior is fundamentally different as the presence of a quay wall perpendicular to the axis of the propeller wash will obstruct its development (figure 5). The figure visibly displays how presence of wall increases scouring at the most vulnerable place- by the very wall itself. Which is the main purpose of scouring assessment- to find out how it would behave, then apply the necessary measures protecting the dam from undermining. Yet it cannot be said that the projected situation in Brouwersdam is the same as the propeller wash next to a quay wall. Such a scouring profile may only be considered as guiding, it is yet to be researched which types of scouring processes are best resembling that of Climate Power Plant.

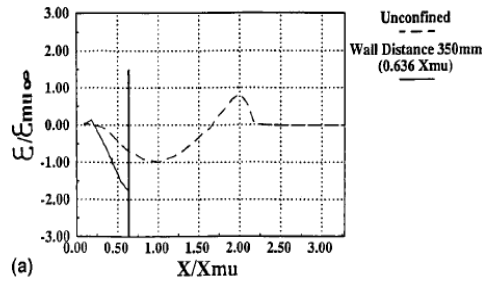


FIG. 6(a). Comparison between Confined and Unconfined Eroded Profiles: Quay Wall at $0.636X_{\mu}$ from Propeller

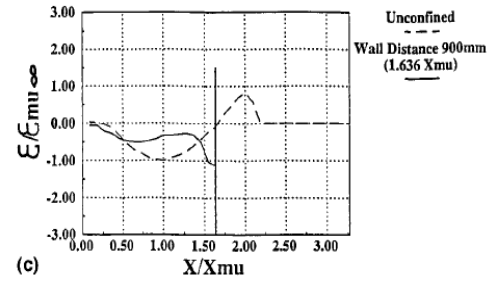


FIG. 6(c). Comparison between Confined and Unconfined Eroded Profiles: Quay Wall at $1.636X_{\mu}$ from Propeller

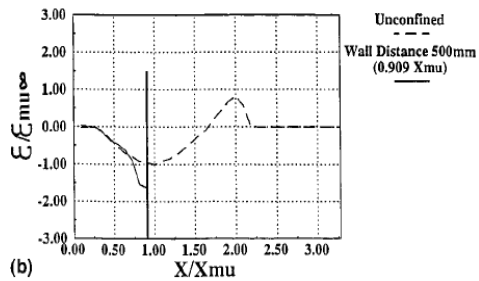


FIG. 6(b). Comparison between Confined and Unconfined Eroded Profiles: Quay Wall at $0.909X_{\mu}$ from Propeller

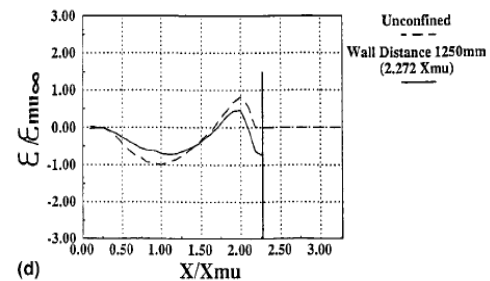


FIG. 6(d). Comparison between Confined and Unconfined Eroded Profiles: Quay Wall at $2.272X_{\mu}$ from Propeller

Figure 5. Bed scour shapes at different proximities between propeller and the wall and unconfined situation. Taken from "Propeller wash scour near quay walls" by G. A. Hamill, H. T. Johnston, and D. P. Stewart.

Given that there is an opening within the dam's structure- a duct enabling flow to Grevelingen, deposition of sediment downstream is also worth investigation to get the full picture of sediment transport which may cause deformations of the quay wall, until a new equilibrium is reached (Roubos & Verhagen, 2007). Entrained material removed from the scour hole may be transported downstream as bed load, or form a mound immediately at the downstream margin of the scour hole (Whittaker & Schleiss, 1984). Such situation would be very much undesired, as bed level decrease on the exterior part and increase on the interior may significantly redistribute the forces acting on the dam and disrupt the steady state.

It could be claimed that the hydraulic structures are the essential pieces in the scouring problems as it decides the flow characteristics. Scouring can be classified according to which type of hydraulic structure flow induces it. While conducting literature review, it seemed the most reasonable to focus on submerged jet and sill and outlets caused scour.

Sill was chosen as usually it is a part of closure dam, in estuaries designed for a two-way flow during floods and ebbs and used to maintain a required water level upstream (Wal et al., 1991). Characteristics resembling that of the Climate Power Plant- designed for flow to and from Grevelingen and requiring to maintain the lake's water level within according margins of +0.05m NAP and -0.45m NAP (Berkel et al., 2018). The flow around sill is characterized by an acceleration upstream followed by deceleration downstream separated by a side slope which causes flow to separate and generate eddy at the bottom until reattachment occurs again and uniformity is restored (Wal et al., 1991). The described flow pattern suggests how the flow would develop within the sluiceway and downstream as the

described flow acceleration and deceleration is almost certain due to afore mentioned law of energy conservation and Bernoulli's principle. Despite it, due to the planned fast switching valve, sill is covering just half of the story- flow occurring while the valves are opened and a steady flow is maintained.

Submerged jet flow would be depicting the other half- moments when the shut valves are opened causing a plunge of water into an ambient medium. Basic features of a jet are diffusion, mixing layers and the extra turbulence due to the decreasing flow velocities (Hoffmans & Verheij, 2011). As explained by Albertson et al. (1948), the jet flow can be distinguished in regions according to their velocities- the potential core and the diffused jet. The former having the same velocity as the efflux and the latter- where the velocity decreases. These high outflow velocities, being a result of hydraulic head differences between the two water bodies, are most likely to cause large shear stresses exceeding the critical value of the bed particles (Chatterjee et al., 1994). Making a contribution to the erosion process which cannot be ignored. Yet how significant this contribution would be is another question remaining to be answered. As explained, such plunging jet flow would occur when the requirement of hydraulic head difference of -0.5m is present, electricity generation is possible and the valve is opened. Meaning that significance of jet scouring depends on the frequency of valve openings. Since such a system is quite novel and not thoroughly studied, the margin of what number of valve openings within the scour development period can be considered of significant influence is under a question mark.

However, this would only matter when designing bed protection. To find a sufficient flow resistance able to withstand frequent plunges and sudden, large volumes of water causing water disturbance. Yet for the area downstream of bed protection, the most important variables are shear stresses, velocities and the local flow resistance. Variables deciding magnitude and extent of scour.

2.5. Sea bed properties and flow resistance

Flow resistance is fundamental for controlling flow hydraulics and fluvial geomorphology in man-made channels or natural streams (Luo et al., 2020). That said, local soil properties ought to be investigated to determine what flow resistance capacity it possesses. The task poses its own challenges and risks of uncertainty as soil types and grain properties differ over the area. Moreover, the flow resistance is strongly affected by roughness and geometry, which depends mainly on arrangement and concentration of coarser elements (Ferro, 2003). The surface roughness is one of the elements deciding the bed shear strength along with flow conditions (Luo et al., 2020). The strength to be compared to the occurring shear stress by the flow exiting the ducts.

Shields (1936) defines flow resistance as the force at which a grain is dislodged from a uniform grain-size bed surface. Such bed homogeneity should be assumed for simplification reasons. The author also emphasizes bed shape and formation significance for particle transport, as formations like dunes and holes etc. form a self-contained system.

It implies that once the flow enters the scour hole, it separates from the main water body and creates a different hydraulic environment within the affected location.

Determination of bed resistance revolves around defining the critical thresholds of velocity and shear stress- acting as stability parameters. In reality, one critical velocity applicable for a wide area does not exist, in fact this velocity differs at each location due to diversity in positioning, protrusion and different loading situations (Roubos & Verhagen, 2007). The differences in protrusion of grains in a bed and, more in general, the differences between the size and shape in a natural material, make an analytical approach of stone stability flawed with uncertainty (Schiereck & Verhagen, 2012). Therefore it is wise to make conservative decisions when carrying out the task.

2.6. Bed protection

A need for scouring assessment and mitigation leads to an installation of some sort of bed protection, to alleviate the subjected stress or move it away from the most liable locations, as bridge piers or toes of quay walls, to protect the structural integrity (Labeur & Uijtewaal, 2019). It enhances the bed resilience or reduces the eroding power (Chiew, 1992). For the resilience to be improved sufficiently and to choose the most optimal solution, it is important to understand the magnitude of the near-bed velocities and bed shear stresses to be expected (Crowley et al., 2020). Defining the threshold at which bed protection would fail and be undermined, exposing the bed layer underneath, forms the design basis. Such a threshold can be defined by a critical velocity- when the current velocities above the bottom protection will exceed a so-called critical value, the protection material will be displaced. By that, a limit state boundary is drawn, within the frames of which, the bed protection can be relied on (Roubos & Verhagen, 2007). Scouring continues until the occurring velocity is below the critical threshold, knowing that, the scouring depth can be defined (Schiereck & Verhagen, 2012).

To design the bed protection system for Brouwersdam, M.H. van Saase (2018) had proposed defining the bed protection using the bed protection guidelines by Rijkswaterstaat:

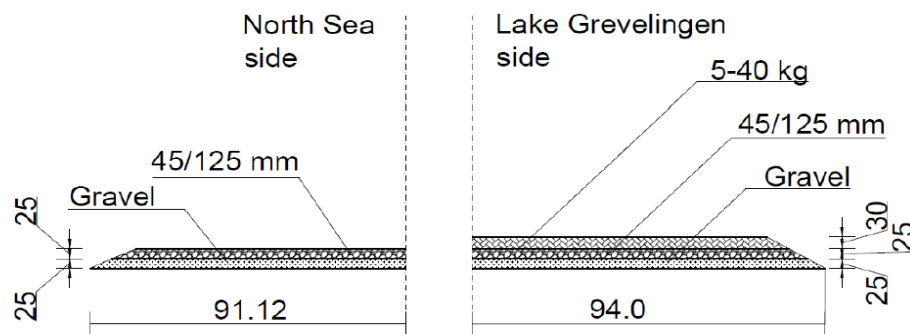


Figure 6. Conceptual Brouwersdam bed protection design. By M.H. Saase adapted from "The Conceptual Design of a Tidal Power Plant in the Brouwersdam"

However, it is beneficiary to first explore and assess scour under assumption that there is no bed protection in place, to learn on the true scouring effect. Insight into the degree of scour without protection is important to the designer, in order to be able to decide whether measures are to be taken (Schierneck & Verhagen, 2012). Total prevention of scour is impossible as was discussed before, some degree of it must be predicted and prepared for due to economic and feasibility reasons (Breusers, 1967). Bed protection should revolve around moving scouring away from the most sensitive areas- the dam- where its occurrence would not result to damage to its stability. As long as the stability of Brouwersdam structure is not endangered, occurring scour is not an issue. In the research article by Hoffmans and Pilarczyk (1995), the authors claim that the length of bed protection depends on the amount of scour allowed- maximum scour depth, the slope of the scour hole, and the geotechnical structure of the soil. With an increasing length of the bed protection- the scour process will be less intense as the turbulence energy of the flow would gradually decay (Hoffmans & Pilarczyk, 1995).

As mentioned, the bed protection must be designed in a way that some extent of scour could be acceptable at the edge of bed protection- the edge scour. Acceptable to a point where no geotechnical instability results in a structural damage to the bed protection, even more so- the hydraulic structure (Broekema, 2020). A task requiring understanding of water flow and bed interaction downstream of designated bed protection, further proving how careful and thorough analysis of bed scour must be.

2.7. *Water hammer effect*

Another matter relating to the explored bed-scour is worth mentioning. In the research description, it was mentioned- use of a fast-switching device, where a Louvre valve is shut within a few moments- 6 s (Maas, van Schaick, & van Berkel, 2018), creates the so-called water hammer effect. A shockwave of energy, occurring when a flowing liquid is suddenly forced to switch direction, propagating upstream. In the specific situation of the tidal power system in Brouwersdam, the created shockwave may damage the duct and the structure of the dam, as the magnitude of water hammer pressure can well exceed the strength of its pipe (Firouzia et al., 2021).

Huge pressure magnitudes, dangerous for the ducts and the whole dam system ought to be contained and mitigated to prevent disastrous events. One parameter is essential in the resulting magnitude of water hammer- the valve closure time. Probability of pipe failure substantially increases with the increase of valve maneuver time. The instantaneous closure of the pipe can create large wave pressures which may lead to sudden collapse of the pipe (Firouzia et al., 2021). In the Climate Power Plant project, the requirement established by the electricity production company is that the valve would close within 10 s to maximize the profit yield (Maas, van Schaick, & van Berkel, 2018). Yet it is questionable whether such a rapid closure is technically feasible. To continue, predicting the pressure values of the water-hammer is imperative so that the mentioned calamities could be prevented. It mostly relies on the flow conditions, Reynolds number parameter in particular, which is decisive: when the Reynolds number and the transient time scale exceed a threshold value,

the flow becomes unstable (Ghidaoui et al., 2005). Having a rapid shutting time and an unsteady flow is unfavorable containing the shockwave nor preventing structural damage, neither assessing bed scour it might cause. Water-hammer is another reason why a frequency of valve closure and opening can be significant for bed protection and scour. Every time a valve is shut, a shockwave is generated, leading to hydraulic disturbance causing additional stress on the bed grains and potentially enhancing scour. The designated bed protection from scouring is assumed to be sufficient to handle the resulting shockwave, yet that is still to be evaluated and confirmed, as the spreading of the shockwave may be significant in shaping the morphology of the bed. Despite that, it is excluded out of the focus of the present research due to being a topic worth time of its own.

3. Methodology

The described concepts and findings of past studies about bed scour in the chapter of Theoretical Framework are to be complemented by calculations of the relevant parameters discussing water flow and scour around Brouwersdam. A scheme for assessing the key factors- velocity, bed shear stress, scour depth was compiled, justified by the concepts of the previous chapter were ties and relations were drawn between these different parameters. The provided method of calculations which then will be put in practice in the chapter of Results will display possible values of the key parameters in relation to time and one another. Although simplified, it should give a glimpse of what could be expected if a tidal power production plant was implemented in Brouwersdam.

3.1. Data collection and modelling

Database of Rijkswaterstaat will be accessed to collect the water level measurements over time, which shall be used as a starting point to assess water level differences, flowing times and directions which will then lead to flow and proceeding calculations. MATLAB- a computing platform for mathematical modelling and visualization will be used for processing the data and performing calculations. It will especially assist when plotting the according data, helping to visualize, interpret the information and draw conclusions.

3.2. What magnitude and scope of velocities will be generated?

The velocities and flow patterns along the length of Brouwersdam, premises of the ducts will differ on a horizontal basis (Broekema, 2020). All mostly due to an array of ducts installed and a trait of a water flow having the largest velocity value in the middle.

For the present research, calculations will take place around a single duct and its efflux, as consideration of all the system would ask for a precise and adequate assessment, requiring sophisticated calculation methods. Thus due to knowledge and time limitations, a single duct unit within the system is worked with.

As mentioned in the subchapter 2.2., the velocity in the system is governed by Bernoulli's law of energy conservation provided below. It allows to understand how the flow is constructed and what the relations between its key parameters are.

$$H = z + \frac{p}{\rho g} + \frac{v^2}{2g} = h + \frac{v^2}{2g}$$

The velocity of the flow is derived from an equation for discharge through submerged orifice, where the key factor is the hydraulic head difference- water level difference between two water bodies, figure 7 below displaying it.

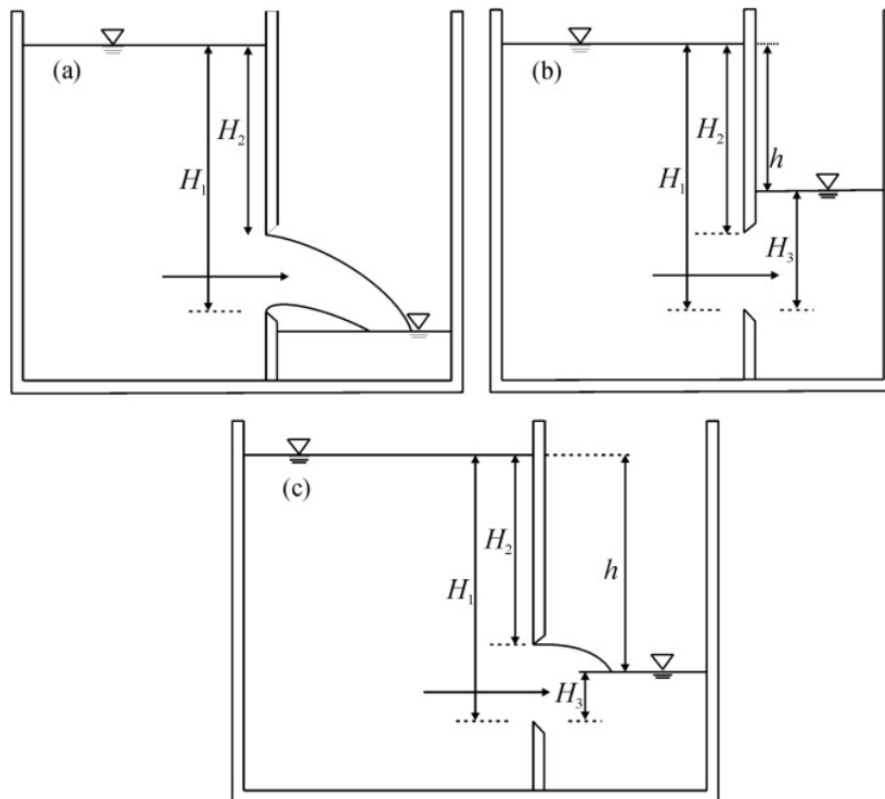


Figure 7. Orifice flow between two basins. Retrieved from "Flow through lateral circular orifice under free and submerged flow conditions" by A. Hussaina, Z. Ahmadb, C.S.P. Ojha.

Orifice discharge formula is:

$$Q = C_Q * A * \sqrt{2 * g * \text{delta}H}$$

C_Q being the discharge coefficient

A cross-section of the flow, equal to the cross-section of ducts

$\text{delta}H$ is the water height difference between the North Sea and Grevelingen

g – Gravity.

In the case of the current research, discharge through submerged orifice is of interest only with respect to the filling of Grevelingen and its changing water level height which is relevant for further calculations of velocity and bed scour development. The velocity from the discharge equation is derived below:

$$u_0 = \frac{Q}{Cq * A} = \sqrt{2 * g * \Delta H}$$

The provided velocity equation depicts its magnitude right before the entry location of the sluiceway. But the efflux velocity is the pivotal one as it results in scouring. In theory, due to law of energy conservation, the total energy of isolated fluid remains unchanged. In practice, hydraulic head losses due to geometry of ducts and friction would result in the loss of energy and velocity as well- which is tied to hydraulic head difference between two water bodies. As the equation above omits hydraulic losses, it will be considered as a point of reference, according to which losses and the final outflow velocity will be calculated. Several types of head loss will be evaluated:

- Entry loss- flow contraction at the inflow.
- Friction loss- occurring due to duct surface roughness and flow turbulence.
- Turbine loss- energy production is requiring a source of energy.

The assessed losses will be included in the efflux velocity calculation:

$$u_{out} = u_0 - \sqrt{2 * g * ((dh_{entry} + dh_{friction} + dh_{turbine}))}$$

Entry losses are to be assessed by the use of:

$$dh_{entry} = \varepsilon * \frac{u_0^2}{2 * g}$$

ε representing the entry loss coefficient, according to the conceptual power plant design by Saase (2018), it is equal to 0.11.

Friction loss results from an interaction between the walls of sluiceway and the turbulent flow:

$$Re = \frac{u_0 * l}{\nu}$$

l representing the sluiceway length, $l = 52.67$ m.

ν - Kinematic viscosity, $\nu = 1.05 * 10^{-6}$ m²/s.

For the distributed head loss calculation, White-Colebrook equation will be applied (Saase, 2018):

$$dh_{friction} = cf * \frac{l}{R} * \frac{u_0^2}{g}$$

cf in the equation is the friction coefficient, $cf = 0.003$.

R - hydraulic radius.

Lastly, turbulence losses are to be assessed. For the matter, the study of Saase (2018), investigating pressure loss by two different types of turbines, will be utilized. The less losses causing turbine loss will be applied to receive higher outflow velocities. It lead to consideration of free-stream turbine, with a loss of:

$$dh_{\text{turbine}} = 0.04 * \frac{u_0^2}{2 * g}$$

The described pressure loss calculations will lead to a decrease in outflow velocity. However, one local loss type was omitted- the exit loss. According to Saase (2018), a flow entering a still water basin, poses an exit loss coefficient of 1. Despite that, the scour development is the result of outflow velocities, thus exit losses are not assessed.

3.3. Velocity at the bed layer

Considering that the velocity of water flow through the duct is proportional to the hydraulic head difference ΔH , an issue of water levels oscillation arises.

To assess it, modelling on MATLAB will be made use of. Tidal variation data of the North Sea will be retrieved from Rijkswaterstaat online database. North Sea tidal variations are totally independent from flow discharged from and to Grevelingen, whereas the water height of the latter- is. Grevelingen level height will rise and decrease depending on the discharge entering and exiting it, this will also affect the velocity. The speed of flow will change proportionally to the absolute value of hydraulic head difference as was mentioned. The change of Grevelingen water level will be modelled on MATLAB, according to the discharge volumes over period of times. Valve closure times will be considered as well, once the hydraulic head difference is under the minimum requirement of 0.5m. Upper and lower boundary limits of the allowed water level fluctuation (figure 8) ought to be adapted into the model as well.

Once the water height difference and velocity fluctuations over time are known, activities downstream the dam can be evaluated. As was explained, the flow decelerates at the exit of the duct, once it ends up in the Grevelingen, where it then begins to mix and dissipate turbulent energy. From literature review it is known that the flow is not uniform neither horizontally nor vertically (Broekema, 2020). Since the significant velocity values are those at the outlet at the duct and at the sea bed, a choice to calculate bed velocity was made, according to the method of Saase (2018), which takes into consideration the distribution of velocity, calculating the location where the mixing flow reattaches to the bed (figure 8). Location considered to be critical for the bed protection.

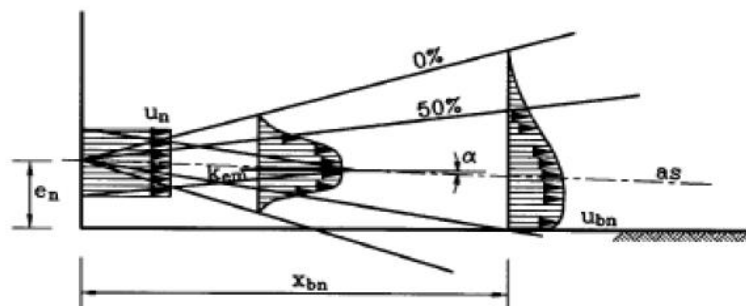


Figure 8. Efflux velocity distribution. By M. H. van Saase, adapted from "The conceptual design of a Tidal Power Plant in the Brouwersdam".

$$x_{bn} = \frac{e_n}{\tan(\alpha + 5.7)}$$

x_{bn} representing the distance over which velocity distributes.

α representing the angle of the flow axis, assumed to be 0 as for the flow discharging straight.

e_n representing the distance from the bed to the flow axis

5.7 degrees angle of the flow approaching the bed (Saase, 2018).

Following the methodology of the same author, bed velocity at the reattachment point will be calculated with a formula:

$$u_b = 2.5 * u_{out} * \sqrt{\frac{d_n}{x_{bn}}}$$

u_b being the flow velocity at the bed layer

u_{out} - the velocity exiting the duct

d_n represents the height of exiting flow- being equal to the dimensions of the submerged duct.

Knowing velocity at the efflux and at the reattachment point, leaves the velocity value within the boundaries of x_{bn} unassessed. It was decided to interpret that the efflux velocity would be kept in that span, even if it should realistically reduce. But because the reduced velocity would turn into turbulence energy, exerting significant stress upon the bed layer, which is unaccounted for under the present methodology, it was decided to compensate it with the higher value of velocity. Moreover, because that is a span closest to the dam, a high velocity is justified for the design of bed protection. Considering the highest possible velocity supposedly affecting the bed layer, is the conservative option for safety. Assumption of the worst realistic scenario ensures the smallest chance of a calamity.

3.4. What magnitude of shear stress will be exerted on the sea bed?

The flow velocity and the shear stress it induces upon its surroundings are closely linked to each other- velocity being the decisive variable for the shear stress magnitude. Over several studies, such as Broekema (2020); Saase (2018); Schiereck and Verhagen (2012) it was that the relationship between velocity and the shear stress is quadratic:

$$\tau = c_f * \rho * u_b^2$$

The formula would display what magnitudes of shear stress are applied upon the bed layer.

c_f stands for the coefficient of friction, depending on the bed roughness.

ρ represents the density of sea water, varying with accordance to the temperature. A fixed value will be considered for a simplicity reason- 1027 kg/m³.

u_b will be the velocity at the bed layer, calculated beforehand.

A slight alternative to the formula above using a drag coefficient instead of friction coefficient will be taken into consideration (Williams, 1993) while all other variables remain similar:

$$\tau = c_d * \rho * u_b^2$$

c_d represents the drag coefficient

The main difficulty with this technique is that the drag coefficient is not a constant and it is therefore difficult to estimate it accurately, according to Dietrich and Whiting (1989) cited in Biron et al. (2004).

In general, coefficients as such represent surface roughness- the resistance to flood flows in channels and flood plains (Arcement & Schneider, 1989). Abundance of varying research on bed roughness and friction factors, offering a range of friction assessment methods was found, e.g. Fenton (2010), Arcement and Schneider (1989). The majority involved intricate calculation procedures. In the manual of COHERENS- an open-source shallow waters modelling system, a drag coefficient equation obtained from engineering practice, was provided:

$$c_d = \frac{g}{C^2}$$

C representing Chezy coefficient.

Chezy coefficient will be assessed by a formula derived by Manning (1891):

$$C = \frac{\sqrt[6]{R}}{n} = \frac{\sqrt[6]{H}}{n}$$

The initial formula requires calculation of a hydraulic radius, which would be fitting for an open channel. Yet because the basin of Grevelingen is far from being one, hydraulic radius is replaced with the water depth, which is adjusted for wide channel situations.

The Manning coefficient n differs per type of soil, the table in the figure 9 will be used to choose the suitable value for the bed material located in the premises of Brouwersdam in pursuit of calculating bed shear stress:

Bed material	Median size of bed material (in millimeters)	Base <i>n</i> value	
		Straight uniform channel ¹	Smooth channel ²
Sand channels			
Sand ³	0.2	0.012	—
	.3	.017	—
	.4	.020	—
	.5	.022	—
	.6	.023	—
	.8	.025	—
	1.0	.026	—
Stable channels and flood plains			
Concrete	—	0.012–0.018	0.011
Rock cut	—	—	.025
Firm soil	—	0.025–0.032	.020
Coarse sand	1–2	0.026–0.035	—
Fine gravel	—	—	.024
Gravel	2–64	0.028–0.035	—
Coarse gravel	—	—	.026
Cobble	64–256	0.030–0.050	—
Boulder	>256	0.040–0.070	—

Figure 9. Bed material types and their characteristic roughness coefficients. Retrieved from "Guide for selecting Manning's roughness coefficients for natural channel and flood plains"

3.5. What is the response of the soil located downstream of the power plant to external forces?

Data and information platform of Dinoloket for the Dutch subsurface will be accessed, to gather information on the bed substrate properties of Eastern Scheldt. The properties will be analyzed and a homogenous soil type will be made use of when performing all the soil relating calculations.

The purpose of the soil related calculations will be to evaluate its resilience and resistance to the effects of the flow induced shear stress and velocities. Critical values of it will be found to determine a threshold at which material deposition could be expected. For the task a method of Shields will be applied which considers a friction force caused by the water on the bed. If the force exceeds a certain critical value the bed starts to erode and grains start to move (Schierreck & Verhagen, 2012). The critical value will be defined by the so-called Shields parameter serving as a stability parameter, which may also become a grain mobility parameter if the actual occurring velocities are used when calculating (Schierreck & Verhagen, 2012):

$$\begin{aligned} \psi_c &= \frac{\text{load}}{\text{strength}} = \frac{\tau_c d^2}{(\rho_s - \rho_w) g d^3} = \frac{\tau_c}{(\rho_s - \rho_w) g d} = \\ &= \frac{u_{*c}^2}{\Delta g d} = f(\text{Re}_*) = f\left(\frac{u_{*c} d}{\nu}\right) \end{aligned}$$

Ψ – Shields stability parameter

τ_c representing critical shear stress

p_s - sand density

p_w - water density

g - gravity

d - characteristic grain diameter, (d50 can be applied)

u^*_{*c} - critical shear velocity

ν – kinematic viscosity

Re – Reynolds number

As represented in the equation, the parameters provides a relation between the applied shear load and the particle Reynolds number. It is noted that the latter parameter is not the usual Reynolds number, as it does not result from the conditions of the flow but indicates whether the grain protrudes whether the grain protrudes into the turbulent boundary layer or stays within the viscous sub-layer (Schierck & Verhagen, 2012). Figure 10 displays a graph used when determining grain stability according to Shields parameter. It draws a relation between Shields parameter to Reynolds particle number.

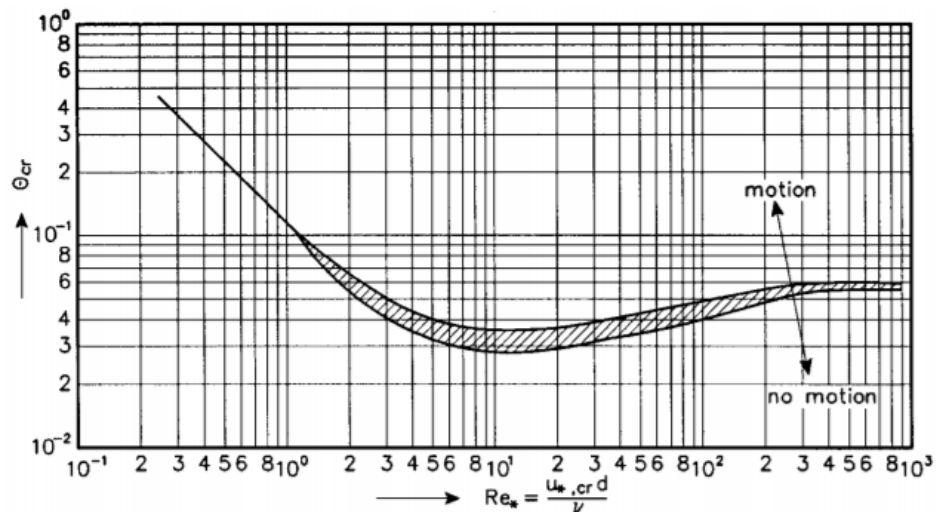


Figure 10. Shields parameter and particle Reynolds number relation graph. Retrieved from "Introduction to Bed, bank and shore protection" (p. 64) by G. J. Schierck and H. J. Verhagen.

An alternative to the table above was developed by Van Rijn (1984), where instead of Reynolds particle number a dimensionless particle parameter (figure 11) is plotted against the very same Shields parameter (named 'Dimensionless shear stress Shields'):

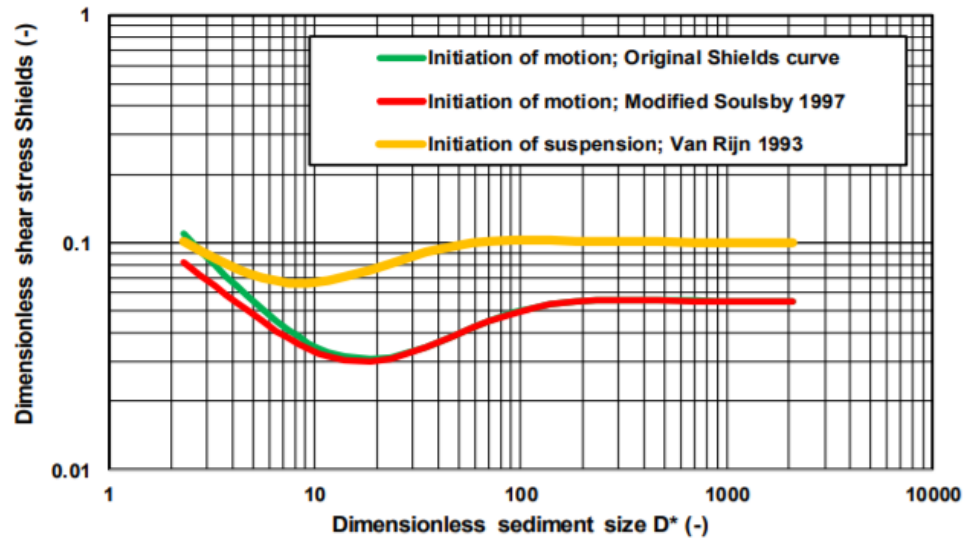


Figure 11. Particles motion determination graph. Retrieved from "Simple general formulae for sand transport in rivers, estuaries and coastal waters" by L.C. van Rijn.

The latter is considered more advantageous as it avoids iteration of u_c (Schierack & Verhagen, 2012). Since the table of figure 11 does not require iteration of critical shear velocity, it will be used in the present research. The involved dimensionless particle parameter is calculated as follows (Rijn, 1984):

$$D_* = D_{50} \left[\frac{(s - 1)g}{\nu^2} \right]^{1/3}$$

D_{50} median particle size

S is the relative density- ratio between sand and water density.

g - gravity.

ν represents kinematic viscosity. $\nu=1.05 \cdot 10^{-6} \text{ m}^2/\text{s}$ (Saase, 2018)

The very same author Van Rijn (2007) states that for fine sand beds, the Shields curve (figure 12 & 13) is not accurate and suggests determining critical shear stress values according to Miller et al. (1977):

$$\tau_{cr} = 0.115 * D_*^{-0.5} \text{ if } D_* < 4$$

$$\tau_{cr} = 0.14 * D_*^{-0.64} \text{ if } 4 \leq D_* < 10$$

Given that it is most likely that the bed in the location of interest consists of a fine sand, the equation will be taken into consideration.

In addition, the very same relation graph and Shields parameter can be used the other way around, when its value determines the conditions of the bed:

Condition of the bottom protection		ψ
Threshold of motion	1) Completely stable	0.030
Occasionally movement some locations	2) Grains go for a roll; in places	0.035
Frequent movement at several locations	3) Grains go for a roll; at several places	0.040
Frequent movement at many locations	4) Grains go for a roll; at almost all places	0.045
Frequent movement at all locations	5) Grains go for a roll; all places not permanent	0.050
Continuous movement at all locations	6) Grains go for a roll; all places and permanent	0.055
General transport of the grains	7) Begin of the march of grains	0.060

Figure 12. Bed protection conditions according to the value of Shields parameter. Retrieved from "Uncertainties in the design of bed protections near quay walls" by A. Roubos and H. J. Verhagen.

Yet this table is more useful for designing bed protection as it represents displacement of large diameter stones (Roubos & Verhagen, 2007). Despite that, Shields parameter can be a useful tool assessing the response of grains to the impact of water flow. It can be of great service when designing an optimal bed protection, indicating what measures suffices or not.

3.6. Equilibrium scour depth assessment

After determining the flow parameters inducing bed scour and the critical threshold at which the soil erodes. Further investigations ought to concern the maximum expected scour depth- the point of equilibrium- depth at which scour can be expected to reach its nominal destination. Schiereck and Verhagen (2012) provide an empirical expression to assess scour behind a bed protection:

$$h_s(t) = \frac{(\alpha \bar{u} - \bar{u}_c)^{1.7} h_0^{0.2}}{10 \Delta^{0.7}} t^{0.4}$$

u with over line standing for the occurring velocity

u_c with over line representing the critical bed velocity

h_o being the original water depth

t a relation of time in hours. A note on scour depth growing in time of power at 0.4

Δ - the triangle- represents the relative density between sand and the sea water.

α is an amplification factor for the velocity, which expresses the disturbance in the flow, hence it is expected to be related to the turbulent fluctuations in the flow (Schierck & Verhagen, 2012). Due to turbulence dissipating over space, the longer the bed protection, the lower value of the factor can be taken:

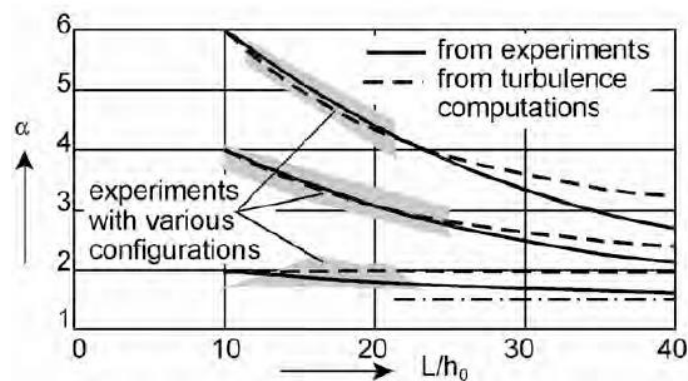


Figure 13. Bed protection length and factor α relation. Taken from "Introduction to bed, bank and shore protection" (p. 108) by G. J. Schierck and H. J. Verhagen.

The table above suggest high amplification factors which could multiply the velocity values and leading to unrealistic outcomes for bed velocities and scour. The factor may differ significantly due to velocity distributions. When defining it for a local value of velocity, for example at a bed level, an equation below is suggested (Schierck & Verhagen, 2012):

$$\alpha = 1.5 + 5r \quad \text{for } \alpha > 1.8 \text{ and } r > 0.07$$

r in the equation stands for relative turbulence:

$$r = \frac{\sqrt{g}}{C}$$

C is the Chezy coefficient for the smoothness of the bed.

Use of Chezy coefficient to define turbulence intensity and then the velocity amplification factor indicates that the latter largely depends on the roughness of the bed surface.

Alternatively, Wal et al. (1991), suggest α to be a function of the geometry of a sill, providing values of the factor in the figure 14:

$\frac{y_D}{y_0}$	$\frac{L_P}{y_0}$	α	
		Bed protection	
		Smooth	Rough
0	10	2.0	1.5
0.3	1 to 15	2.5	2.0
0.6	3	3.2	3.0
0.6	10	2.9	2.5

Figure 14. Velocity amplification factor as a function of relative sill height, bed protection length and bed roughness. Taken from "Scour Manual" by M. van der Wal, G. van Driel and H. J. Verheij

The author suggests relation of y_d/y_0 in cases of submerged outlets as well. Obviously, no sill is planned to be installed, thus y_d/y_0 relation is 0.

The different means of amplification factor assessment will come useful in the results phase, once concrete values are known, allowing to determine the suitable way and an according α value.

$h_s(t)$ - the maximum scour depth as a function time would result in an exponential curve without a definite flattening. The true equilibrium depth, where a scour could be assumed to have reached an asymptotic state, can be calculating using the very same guidelines of Schiereck and Verhagen (2012):

$$\left. \begin{aligned} u_c &= 0.5 \alpha \bar{u}_s \\ \bar{u}_s (h_0 + h_{se}) &= \bar{u} h_0 \end{aligned} \right\} \rightarrow \frac{h_{se}}{h_0} = \frac{0.5 \alpha \bar{u} - \bar{u}_c}{\bar{u}_c}$$

In the end of this further investigation of scour development, a maximum scour depth and a period of time required for its development can be attained. It will assist on anticipating scour and planning construction process, maintenance routine accordingly. Also, it provides important information for bed protection design. The final thing worth evaluation is the length of scour affected bed layer or the size of the scour hole. A method presented by Wal et al. (1991) will be applied:

$$L_s = 0.5 * h_{se} * (16.3 - \cot\beta) - 4.35$$

h_{se} is the maximum scour depth.

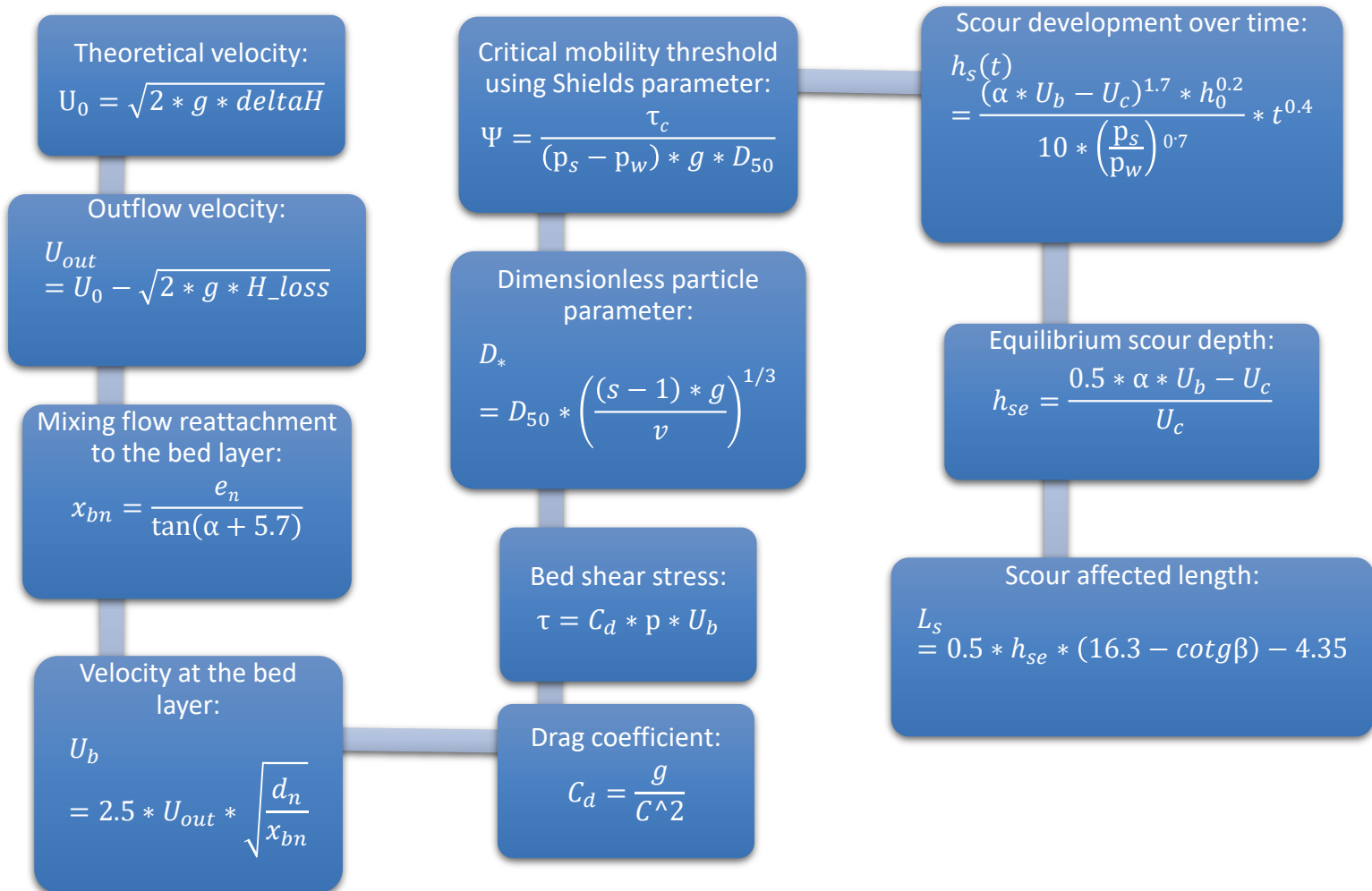
$\cot\beta$ angle of the scour hole slope, requiring an equation for calculation as well:

bulk density of fine sand	critical initial slope of scour hole	phenomena
very loose	1 : 2.25	flow slide
loose	1 : 2.00	flow slide
dense	1 : 1.75	sliding
very dense	1 : 1.50	sliding

Figure 15. Critical initial slopes of scour hole. Retrieved from "Scour Manual" by M. van der Wal, G. van Driel and H. J. Verheij.

3.7. Calculation process scheme

The just described scour assessment procedure is displayed below in a concise scheme. The visualized scheme represents the calculations undertaken and analyzed in the results chapter. For clarity and clear comprehension, the schematized step-by-step methodology shows direct links between different parameters calculations and can be conveniently investigated and applied:



4. Results

The compiled bed scour assessment scheme will be applied evaluating the flow conditions and the response of the bed in the area of Brouwersdam. The obtained results findings will be analyzed and discussed, conclusions will be drawn aiming to answer the research questions and the main topic of the research: how would the morphology of the bed around the barrier change if a tidal power plant was implemented.

4.1. Varying water levels and valve positions

First task to do is: modelling the change of Grevelingen water level against the tidal fluctuations of the North Sea. North Sea water level measurement data of a period April 2nd –April 29th was retrieved from Rijkswaterstaat online database. Water height measurements were taken every 10 minutes, resulting in a significant set of data. As for the Grevelingen water table height change, it was organized by discharge increasing or reducing it, within the limits of maximum and minimum water level heights and limits of minimum hydraulic head difference. If these limits were crossed, Grevelingen water level would be maintained, indicating shut valves forbidding flow. Water level fluctuations of the interacting water bodies are displayed below, two graphs for two time periods:

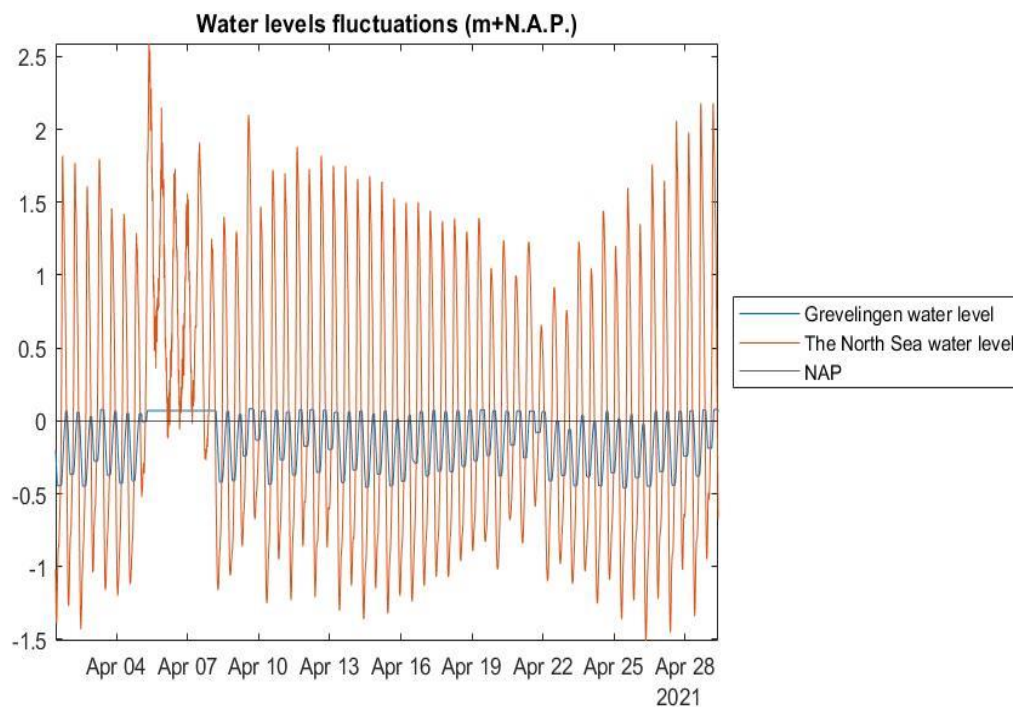


Figure 13. Water level fluctuations April 01-29 2021

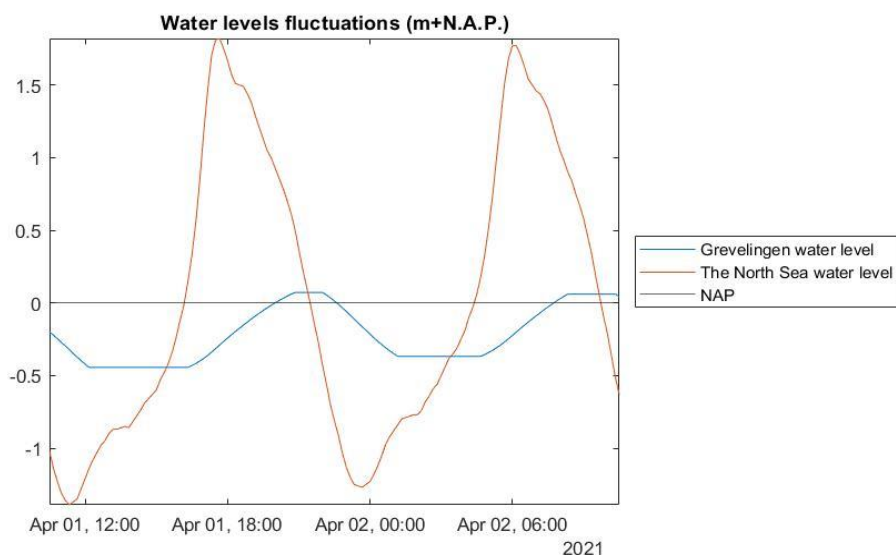


Figure 17. Water level fluctuations April 01-02 2021

By using the readings of the computed discharge or velocity values, flow times and durations can be found. If boundary requirements of minimum hydraulic head difference and Grevelingen water level limits are met, absolute values of discharge and velocity exceed 0. A graph displaying valve and flow status is provided in figure 18:

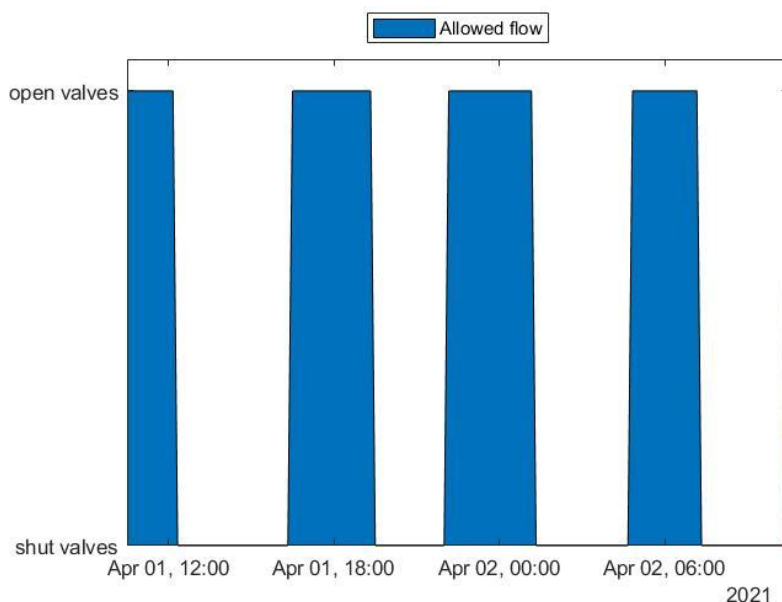


Figure 18. Flow monitoring valves position during April 01-02 2021. The colored area display when the valves are open and flow is enabled.

Total open valve times when flow occurs and electricity is generated can be computed as well. During the total time period of analysis, April 1st 10:30 to April 29th 9:10, flow is allowed for in total of 16130 minutes, which is approx. 269 hours. A table below overviews cumulative durations of open and closed valves over several time periods and open valve ratio over the total time periods.

	Open valves times in hours	Closed valves times in hours	Open valve ratio (%)
28 days (total analyzed time period)	268.83	396.3	0.4
7 days (April 1st-8th)	46	122.2	0.27
1 day (April 28th)	9.2	14.83	0.38

Figure 19. Open valve durations on different time periods

The provided open and shut valve times may differ on different time periods and calendar days, all due to the varying water level differences of the North Sea and Grevelingen which directly influences opening and closing of valves controlling flow.

Durations and frequencies of valve openings and closures and frequencies are important determinants for scouring as the longer is flow enabled, the more severe scouring it may result in. Whereas frequency of valve opening may indicate how significant plunging jet may be to the overall scour development process.

4.2. Duct outflow velocity magnitudes

The first objective in line with the research sub-questions is the determination of the occurring velocity values, which has significant weight in determining the other research topics. The MATLAB model, arranged according to the methodology described, results in the graph of velocity magnitudes:

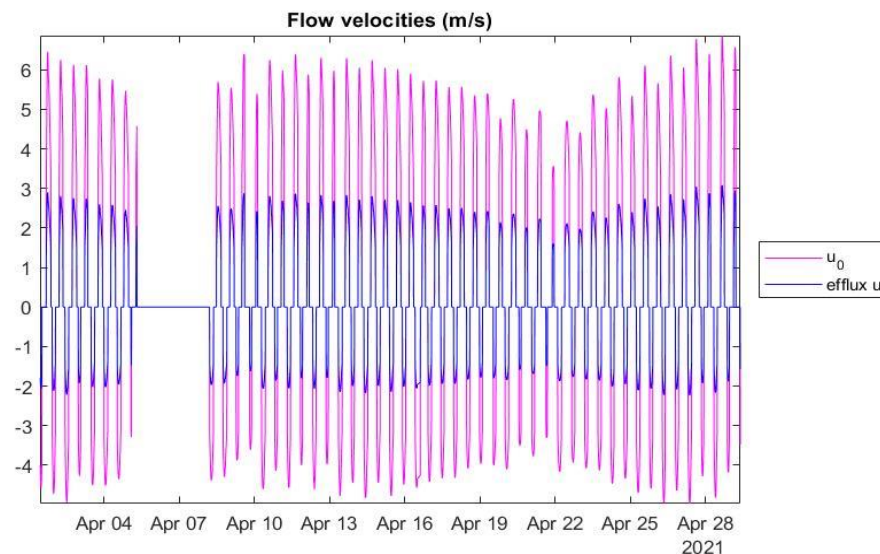


Figure 20. Velocity values occurring at the outflow of a duct.

Positive values in the graph display velocities occurring in the direction of when flow is entering Grevelingen, negative values- when exiting. Head losses significance can be noticed, comparing the magnitudes of the displayed velocities, which differ approximately 2 times. Particular averaged hydraulic head loss data is presented:

Total hydraulic head loss (m)	Local entry loss (m)	Distributed loss (m)	Turbine loss (m)
0.317	0.115	0.16	0.042

Figure 21. Hydraulic losses

It can be seen in figure 20 that in the period of 5th-8th of April, velocity is equal to 0- meaning the valves are closed. Comparing figure 20 graph to figure 16, it shows that in the mentioned time period, the North Sea tide level is outstandingly high while the level in Grevelingen is remaining stable- just as in the last graph. This can be explained by the water level reaching its upper boundary in the lake yet still significantly lower than of the North Sea, which would result in continued increase in the lake water level but is denied due to closed valves- holding flow velocity at 0 in the time span. It proves how opening and closing durations depend on the time and date of measurement and height difference fluctuations.

The calculated outflow velocities reach maximum values: of up to 3.1 m/s when entering Grevelingen and 2.2 m/s when entering the North Sea. The average velocity of flow exiting into the lake is 2.18 m/s, while the mean exit velocity to the North Sea is- 1.76 m/s.

These velocities do not display those that affect the sea bed and deposit the grain. As was discussed, the flow decelerates upon exiting the ducts, thus an according bed velocity ought to be calculated. Within the mixing area next to the dam structure where the most hydraulic activity takes place and turbulence is the highest, the efflux velocity can be applied when designing bed protection, for the reasons already explained. As for downstream, a reattachment location ought to be firstly calculated:

$$x_{bn} = \frac{e_n}{\tan(\alpha + 5.7)} = \frac{6.22}{\tan(5.7)} = 62.3 \text{ m}$$

e_n was set to be between middle of the flow axis (-5.62+NAP) and the sand bed level (-11.84+NAP), resulting in a flow reattachment point of 62.3m downstream of the duct.

To calculate the bed velocity, an average value at outflow will be used- to anticipate the most usual conditions:

$$u_{b\text{lake}} = 2.5 * u_{\text{out}} * \sqrt{\frac{d_n}{x_{bn}}} = 2.5 * 2.2 \frac{\text{m}}{\text{s}} * \sqrt{\frac{8.24\text{m}}{62.3\text{m}}} = 2 \text{ m/s}$$

$$u_{b_{sea}} = 2.5 * u_{out} * \sqrt{\frac{d_n}{x_{bn}}} = 2.5 * 1.76 \frac{m}{s} * \sqrt{\frac{8.24m}{62.3m}} = 1.6 \text{ m/s}$$

u_{blake} representing water flow into the lake, $u_{b_{sea}}$ – flow out of Grevelingen into the North Sea. These velocity values can be expected once the flow regains uniformity, inducing stress upon the bed and washing out scour hole at the edge of the bed protection. Figure 22 below provides a graph of bed velocity change over time:

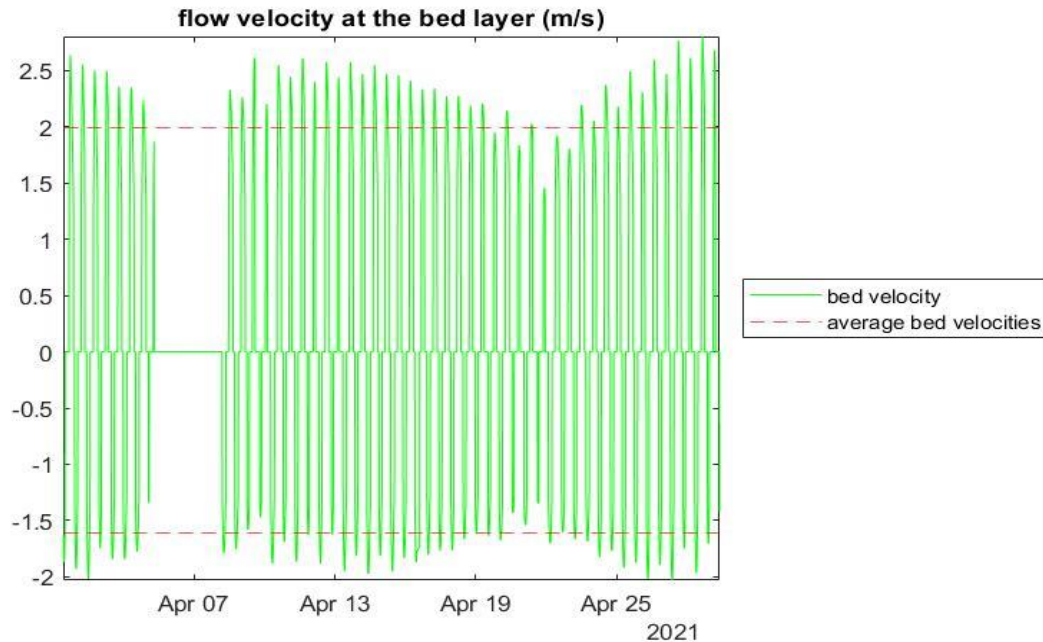


Figure 22. Velocity magnitude at the bed layer.

It can be seen that bed velocities are just slightly lower than those at the exit of the duct. The velocities can be better compared at a smaller time sample (figure 23). It suggests that in the part of x_{bn} until the reattachment point, the mixing turbulent flow losses negligible amount of energy as the velocity reduces only within decimal amounts.

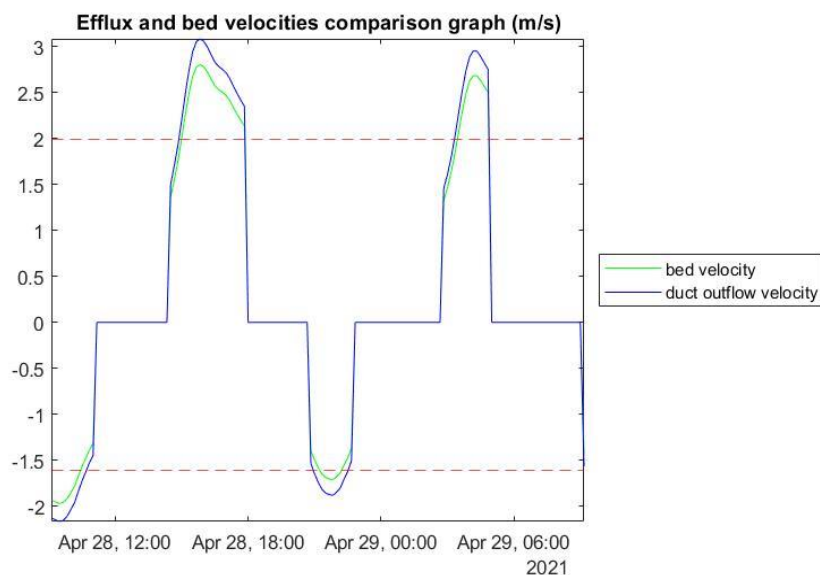


Figure 23. Velocities occurring at the exit of the duct and at the sea bed after reattachment.

4.3. Bed shear stress

Continuing with the designed research frame, after the velocity values are known bed shear stresses can be computed. These will display what stress is induced upon the bed particles which can then be compared to the critical shear stress defining the flow resistance. In order to design sufficient bed protection.

Following the equation calculating bed shear stress, first should be determined the bed soil type which will then lead to selecting an appropriate friction coefficient. Dinoloket data base of stratigraphy measurements was accessed to find out which soil type is characteristic for Grevelingen and the North Sea. Multiple substrate data profiles taken at the location optimal for Tidal Power Plant (Saase, 2018). The selected samples were at the locations where scour could be expected- on both sides of the dam. All the samples (profiles of which are attached in the Appendix) had shown that sea bed consists of fine to medium sand, of up to 12-20m depths. It will be considered further on.

As explained in the Methodology section 3.3., according to the characteristic soil type for the area, shear stresses will be calculated with an according drag coefficients. According to Wentworth (1922) grain size classification, the range of grain size for fine to medium sand is 0.2-1 mm, leading to Manning's roughness coefficient values in the range of 0.012-0.026 (figure 9). As the soil varies over the area, boundary values will be used to find the Chezy coefficients for fine and medium sands:

$$C_{\text{fine sand}} = \frac{\sqrt[6]{11.84}}{0.012} = 125.8 \sqrt{\text{m/s}}$$

$$C_{\text{medium sand}} = \frac{\sqrt[6]{11.84}}{0.026} = 58.1 \sqrt{\text{m/s}}$$

A fixed water depth was chosen to be at a level of -0.00m+N.A.P. which in reality varies and would influence the value of Chezy coefficient. This should be taken into consideration when designing.

All the input data to find the drag coefficient is now known:

$$C_{d\text{fine}} = \frac{9.81}{125.8^2} = 6.28 * 10^{-4}$$

$$C_{d\text{medium}} = \frac{9.81}{58.1^2} = 2.9 * 10^{-3}$$

The calculated drag coefficients enable the assessment of shear stress affecting the bed particles. Yet another MATLAB model was compiled to calculate the shear stress by using the varying bed velocities over the explored timeline.

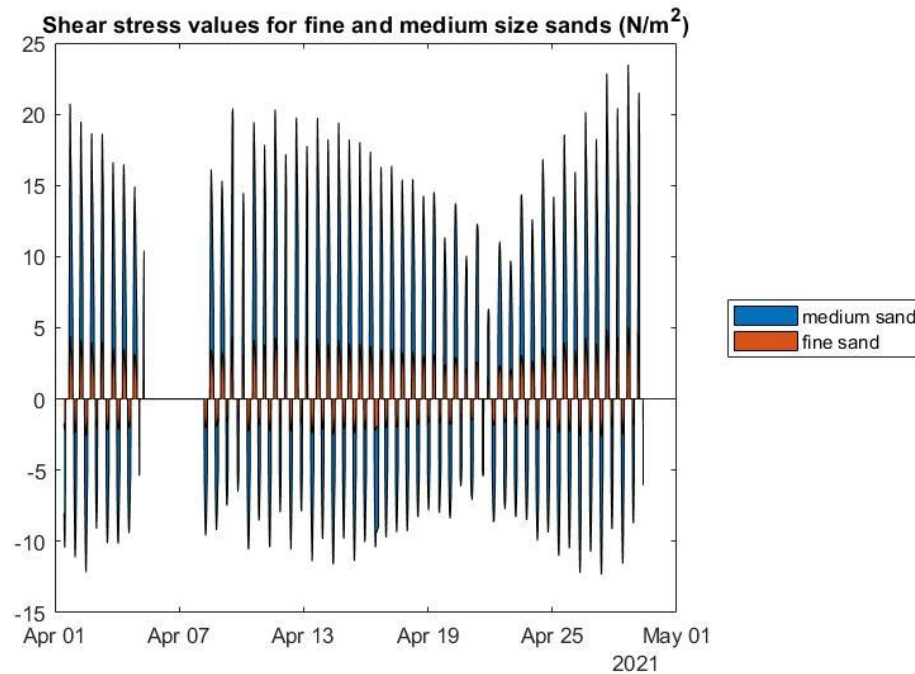


Figure 24. Shear stress exerted upon sea bed graph.

Positive values represent those stresses occurring within the lake, once the flow is entering it, while negative values- those stresses occurring on the sea side. Maximum magnitude of shear stress in the graph reaches 23.46 N/m²- projected on the lake side. Largest value on the North Sea bed tops -12.3 N/m². The graph above shows all the shear stresses occurring during the month of April comprising a clear display of shear stress differences between medium and fine sands. To clearly present it, a graph on a shorter time period is provided, figure 25:

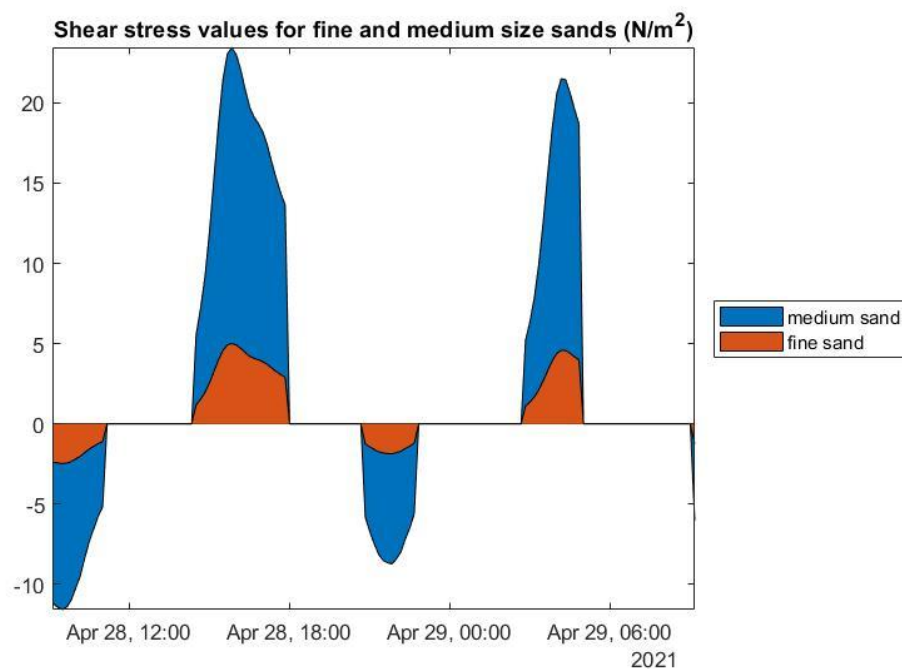


Figure 25. Occurring shear stress values for fine and medium sands during April 27-29th 2021.

The displayed shear stresses represent that of boundary drag coefficients. Therefore, the varying sand grain sizes and compositions should be subjected by shear stresses within the colored range. It allows to orientate within potential shear stress values and draw margins for expected magnitudes, coming useful for the next task of assessing bed particles reaction when a flow resistance will be compared to the impact of shear stress.

4.4. Bed sediment response and deposition

Knowing the potential magnitudes of shear stress, evaluation can be performed for sea bed particles stability or mobility if they are deemed to be displaced. The method described in methodology section 4.4 will be applied with the known input data.

The task, first of all, requires determination of dimensionless grain parameter D^* . D_{50} in the equation will be found using the tabulated median grain sizes in figure 9. That being 0.2 and 1 mm.

$$D_{*fine} = 0.2 * 10^{-3} * \left(\frac{\left(\frac{2000}{1027} - 1 \right) * 9.81}{(1.05 * 10^{-6})^2} \right)^{\frac{1}{3}} = 4.07$$

$$D_{*medium} = 1 * 10^{-3} * \left(\frac{\left(\frac{2000}{1027} - 1 \right) * 9.81}{(1.05 * 10^{-6})^2} \right)^{\frac{1}{3}} = 20.35$$

The received parameters results indicate that different methods to determine grain status of motion ought to be applied. As was discussed in the methodology section 3.4., Shields curve is not ideal for fine sand particles motion determination. The critical shear stress threshold for fine sand will be calculated with the provided equation:

$$\tau_{crit} = 0.14 * (D_{*fine})^{-0.64} = 0.14 * 4.07^{-0.64} = 0.057 \frac{N}{m^2}$$

As for the medium sized sand type, Shields curve will be made use of, leading to calculation of Shields parameter. The maximum value of modelled shear stress will be used as it describes the worst realistic conditions potentially depositing sediment

$$\Psi_{medium\ sand} = \frac{23.46}{(2000 - 1027) * 9.81 * 0.001} = 2.46$$

Both values, although from different point of reference, display that sand is definitely becoming suspended and removed from its initial location, leading to an erosion. The former value of τ_{crit} is indicating the threshold at which particles are initiated in motion,

when shear stress occur in the magnitudes as in figure 24 or 25, wash-out of sand sediment would be instant. $\Psi_{medium\ sand}$ parameter is indicating similarly, yet in another way- the Shields curve must be considered as a point of reference. If the measured Shields parameter is under the curve the particle stays static, if over- it gains mobility. Such value of $\Psi_{medium\ sand}$ as was found would lead beyond the grid of the graph provided (figure 11), unconditionally grains would be displaced at such values.

It shear stress and flow resistance calculations showed that the sand bed would get eroded unconditionally. The provided and trialed method of flow resistance evaluation can be of great service when designing bed protection as the protecting material dimensions can be tested against those of the flow to find whether it would be removed or hold its ground against the external forces pressure. The Shields method can also serve in a way of helping to evaluate what dimensions of bed resistance to flow are required. Speaking of the presently analyzed case of indicated wash out of sand, it would continue uncontrollably eradicating the bed completely. In the Theoretical Framework section 2.3. it was discussed that, with the increasing scour depth, velocity would gradually reduce and along with it the shear stress which eventually would be unable to continue the wash out. That is when the scour hole reaches an equilibrium phase. In the next section, equilibrium depth will be assessed, leading to maximum depth of scour hole and time it needs to develop.

4.5. Scour development and equilibrium depth

The bed change assessment process will be rounded off by evaluating the development of the scour hole in depth over time. Above all, the location of the expected scour hole should be noted. The assessed scour hole will not occur directly downstream of the duct nor at the flow reattachment point as those locations will receive resistance enhancing bed protection. Scour is expected to appear directly downstream of the bed protection, where the sand bed is exposed to the flow.

The location of the scour hole was clarified, therefore the development evaluation can be performed using the method described in section 3.5 of Methodology chapter. Almost all the input data is already known, except for the amplification factor α and u_c - critical velocity at which grains are initiated in motion. The former can be found using the table in figure 16. Yet it is a topic of discussion which curve should be taken.

According to recommendations of Schiereck & Verhagen (2012), in the case of an outlet structure that discharges into a large body of water, there are no clear vertical and/or horizontal constriction dimensions, the amplification factor can be approximated to a value of 4 for a bed protection being 10ho. In the present case, that would be 118m which would seem a safe length for the stability of the dam to not suffer. Despite that, such a large velocity factor would multiply the velocity magnitude, which would be way over realistic bounds. The equation for a local α value, using relative turbulence deemed it to not suffice the requirements. Using the table in figure 17 where the factor is defined as a geometrical function provided adequate a value of 2, considering the bed to be smooth, $y_d/y_o=0$; and $L_p/h_o=10$. This value will be applied.

To acquire the critical velocity value, Shields parameter will be of service. In this case, the upper boundary of medium grains will be worked with, following the logic that if larger grains are washed out- so will be the smaller ones. Moreover, as can be seen in the stratigraphy data in the Appendix, fine sand in the most cases is at the top layers, whereas deeper parts consist of larger grains. The critical velocity of medium sand will be found using the values of the Shields curve.

For dimensionless grain parameter of medium sand, which is 20.35, the Shields parameter at the 'initiation of motion' red line location on figure 11 is equal to 0.03. An equation for critical velocity can be derived from Shields parameter and shear stress equations:

$$\Psi_{\text{shields}} = \frac{C_d * p_w * u_c^2}{(p_s - p_w) * g * d}$$

$$u_c = \sqrt{\frac{\Psi_{\text{shields}} * (p_s - p_w) * g * d}{C_d * p_w}} = 0.31 \text{ m/s}$$

The calculated value indicates that medium sand grains would initiated into motion at 0.3m/s threshold.

Now that all the input data for $h_s(t)$ was acquired, the value of interest can be found. Calculated average bed velocities and water height at N.A.P. will be used respectively, scour development in time will be assessed for both sides of the dam:

$$h_{\text{slake}(t)} = \frac{(2 * 1.98 - 0.31)^{1.7} * 11.64^{0.2}}{10 * \left(\frac{2000}{1027}\right)^{0.7}} * t^{0.4} = 0.93 * t^{0.4}$$

$$h_{\text{sea}(t)} = \frac{(2 * 1.6 - 0.31)^{1.7} * 11.84^{0.2}}{10 * \left(\frac{2000}{1027}\right)^{0.7}} * t^{0.4} = 0.62 * t^{0.4}$$

The defined function of scour depth development in time shows the rate of scour hole deepening. Yet it does not determine the equilibrium depth at which scour deepening can be expected to stop. The maximum depth is to be calculated separately:

$$h_{\text{se}} = \frac{0.5 * \alpha * u_b - u_c}{u_c} * h_o$$

$$h_{\text{se}(\text{lake})} = \frac{0.5 * 2 * 1.98 - 0.31}{0.31} * 11.64 \approx 62.7 \text{ m}$$

$$h_{se(sea)} = \frac{0.5 * 2 * 1.6 - 0.31}{0.31} * 11.84 \approx 49.3 \text{ m}$$

As the scour development function and the maximum depth are known, an estimation can be made for how long will it take for scour holes to fully develop. Figure 26 displays the curves of scour holes development.

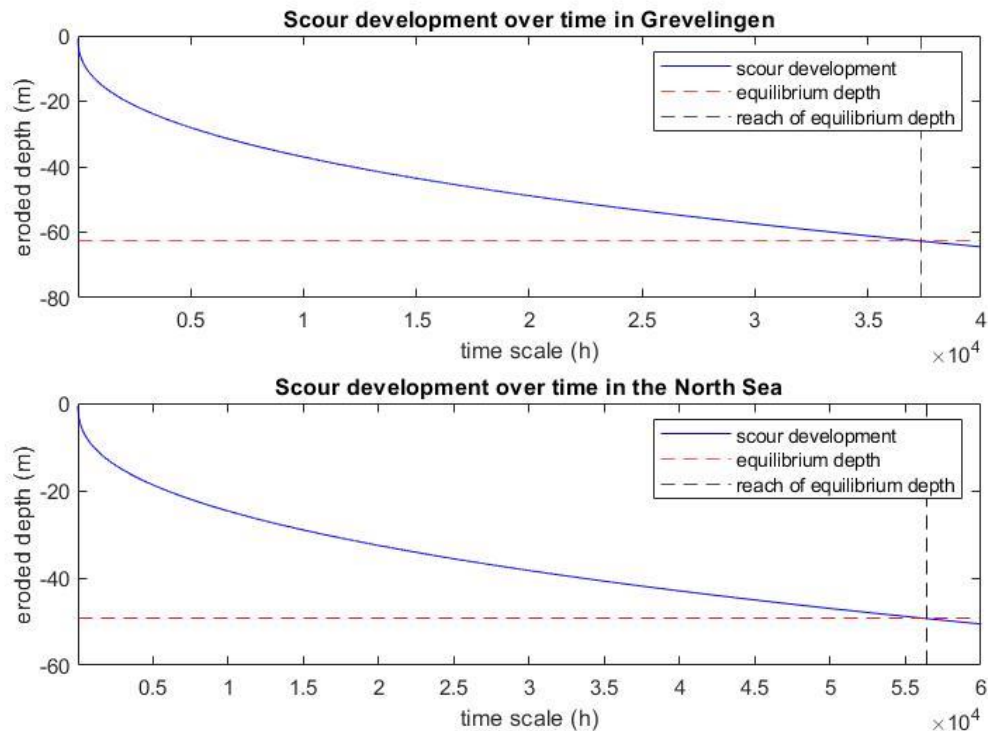


Figure 26. Scour development in relation to time

MATLAB modelling showed that the maximum scour depths would be reached in:

- Approx. 4 years on the side of Grevelingen.
- Approx. 6 years (65275 hours) on the side of the North Sea.

The values above are time periods of open valve time. But it is important to consider that scour development will not be continuous, meaning, that the valves will not be open at all times denying occurrence of flow. For that, a ratio of open valve time will be applied, as was provided in figure 18. The flow time ratio found for the period of April will be used under assumption that a similar ratio will be similar in the future. Hence, the total time for scour development can be found:

$$T_{\text{total}} = \frac{t_{\text{scour}}}{0.4}$$

$$T_{\text{total}_{\text{lake}}} = \frac{37322 \text{ h}}{0.4} = 93305 \text{ h} \approx 10.6 \text{ years}$$

$$T_{\text{total}_{\text{sea}}} = \frac{56382 \text{ h}}{0.4} = 140955 \text{ h} \approx 16 \text{ years}$$

The times to reach the maximum depths are quite lengthy, it can be associated with a decreasing rate of scour, as visible in the graphs of figure 25, and the decreasing velocity with an increase of scour hole depth.

The scour assessment will be finished by estimating the length of bed layer affected by scouring:

$$L_{\text{scour}_{\text{lake}}} = 0.5 * 62.7 * (16.3 - 0.67) - 4.35 = 485.7 \text{ m}$$

$$L_{\text{scour}_{\text{sea}}} = 0.5 * 49.3 * (16.3 - 0.67) - 4.35 = 380.9 \text{ m}$$

The affected spans seem quite large, yet not unrealistic. According to a Scour Manual by Wal et al. (1991), possible scour hole lengths are limited to $L_s = 8 * h_{se}$ for shallow scouring ($h_{se} < 40 \text{ m}$) and $L_s = 10 * h_{se}$ for deep scour holes. Furthermore, assuming that the scour hole would be concentrated within a small width, yet deep in size, requires some sort of an obstacle downstream of it blocking the flow. Since flow is not constricted and proceeds downstream freely, it seems logical for the scour affected area to be as extensive as calculations had shown.

Having the length of scour affected area estimated, the scour assessment can be considered complete. Known equilibrium depth, slope of the hole, affected area and its development in time allows to plan and prepare for construction phase and maintenance, as the undermined soil around the bed protection will require reinforcement.

5. Discussion

The present research and its findings are worth discussing, interpreting the results and contemplating on the research process, method and its findings. In addition, how do the stated research questions align with the main research objective and purpose?

The results can be discussed in an orderly sequence similar to the Results chapter. Starting with the water level height oscillation of the two water bodies and how it influences opening and shutting of valves, the defined water height limits for Grevelingen is the main factor limiting energy production. The defined bounds are limiting energy production as it forces the valve to be closed. In fact, it is not the valve that monitors the flow and energy production but the water level of Grevelingen, whereas valves are just tools for flow discontinuance. Figure 18 provides a table for open and shut valve times over different time periods. Over the whole month of April, valves are open only 40% of the total time. It is already a quite significant amount for electricity generation, yet there is available room to increase the production yield. According to the graph of figure 16, displaying water level fluctuations, it is clear that flow valves are shut not due to insufficient hydraulic head difference- the North Sea water level greatly surpasses that of Grevelingen as its upper boundary limit is reached. If Grevelingen water level restrictions were to be reviewed and increased, the remaining electricity generation potential could be exploited.

Speaking of the sluiceway exit velocity, in regards to bed scour, it is only relevant as far as determining the bed velocity, which puts stress upon the bed grains. However, the part worth attention is the difference between the velocity upon entering and exiting the ducts- the head loss. Head losses as they were assumed and considered, lead to halved efflux velocities, which is favorable for bed protection design and scour damage mitigation. If according duct design choices are made, efflux velocity can be reduced even further. Yet it is important to not compromise electricity production as the turbine efficiency is proportionate to the hydraulic head difference. Thus, loss increase should be investigated at or downstream of the production system. Saase (2018), had explored local hydraulic losses resulting from the turbine, where a bulb turbine leads to more loss than the free-stream. In the current research the worse conditions were considered for worse outcomes but a bulb turbine, inherently resulting in more hydraulic head losses, would reduce outflow velocity.

The calculated velocity magnitudes at the bed layer were only slightly lower than those at the efflux. That is probably due to the chosen method for calculations yet a relation between efflux velocity and bed velocity is undoubted. Therefore, head losses in effect are scour damage alleviators. Coupled with other mitigation measures, it could contribute to the desired goal of bed protection.

Resolving the question of bed velocity allowed to sequentially continue to the assessment of the shear stress applied on the bed grains. The used bed velocity value and drag coefficients determining the roughness of the bed conclude that the evaluated stress is for the bed layer spanning downstream of bed protection. The assumption was made that an effectively flow resisting bed protection would be in place. In such case, investigating shear

stress on a surface which will be covered by bed protection is excess and unnecessary. Unnecessary also due to the complex hydraulic conditions of area at the exit of the sluiceway: high turbulence, converging and diverging flows vertically and horizontally would have made it a tedious task. Hence, it was decided to focus on the shear stresses downstream of the bed protection, where it would have influence upon the surface.

The results showed shear stress inverse proportionality to the grain size and Chezy coefficient which decide the one of the variables in the shear stress equation- the drag coefficient. Higher drag coefficient resulted in higher shears stress values. Meaning that shear stresses may vary greatly, as it varies in figures 24 and 25. This indicates a flaw of assessing shear stress in such way as on a large bed area grain sizes and types may differ significantly, so will vary the drag coefficient and the resulting shear stress. This should be kept in mind as it may alter consequent calculations.

A similar flaw is common for the calculations of bed grain entrainment, as it only covers grains of particular size. Yet the chosen way to use the dimensionless particle diameter instead of Reynolds particle number is advantageous as it allows avoiding iterations of critical shear velocity- this would be required if bed protection were to be designed. This proves that Shields method is a handy parameter, for both: grain mobility evaluation and definition of the critical stability threshold.

The final piece of the Results chapter comprised of scour development depth in relation to time. The founded results of projected depths seems reasonable, comparing to the study of Broekema (2020) who observed bed scouring at the Eastern Scheldt Storm Surge Barrier, where it reaches depths of 40m from the bed surface and still continues as the measured velocities in the hole is still reaching 2 m/s. In the method of evaluation, the most debated piece would be the amplification factor- it was chosen to be fixed at a value of 2 but according to Schiereck and Verhagen (2012): for projects of importance, experiments using a scale model will be necessary, as the factor can lead to a substantial change in development in time and equilibrium depth outcomes. Moreover, another element which can lead to substantial change in results is the chosen sand density, which can vary from 1500 kg/m³-2000 kg/m³ reaching up to 2650 kg/m³ in the study of Saase (2018) and the work of Wal et al. (1991). These parameters are applied in the critical velocity and scour development in time calculations, therefore should be overthought before applying.

Scour development over time trends and the required time to reach maximum depth may pose doubts and questions. First of all, the scour development time graph shows logarithmic curves of scour depth development, which means that the rate of scouring decreases over time. Such trend can be justified by the scouring characteristics explained in the Theoretical Framework. The scouring is rapid at the initial phase, where 20-30 m depths are reached within a year (figure 26), can be justified by the positive feedback phenomenon suggesting that scour causes scour. The scour hole slope amplifies the local erosion and thus the process self-induces. The decreasing scouring rate can be justified by the decrease of velocity within the hole, as it loses energy by the time it reaches the bottom. Moreover, in the deeper layers the soil is much more consolidated due to grain weight from above, and does not protrude into motion as easily- it is more resilient to the scouring forces. Lastly, the main factor increasing the time to reach the equilibrium depth are the

valves, which, at least for the month of April, were open 40% of the time. Therefore, if similar opening rates are kept in the future, the development process will be slow.

Lastly, the bed span affected by scouring results in large values. Although it fits the guideline values suggested by Wal et al. (1991), it is worthy of additional elaboration. It ought to be understood that the flow, once it exits the ducts and proceeds downstream, endures no restrictions whatsoever. As it would then pass over the bed protection, onto sea bed where scouring is acceptable it still behaves as an unrestricted flow. As no vertical constrictions disturb and contain the water flow, it is freely dissipating over the vast space of Grevelingen. Which is favorable, since if the scouring length was attempted to be restricted, it most likely would result in deeper scouring, and larger scour hole slope. It also refutes the possibility of mound formation suggested by Whittaker & Schleiss (1984)-intense hydraulic environment and absence geometrical constrictions does not create the necessary conditions to capture and sustain sediment.

In case it is desired to reduce the extent of scour affected bed area or reduce the scouring hole depth and its slope, maximizing bed protection roughness could be one of the measures to achieve it. Rougher bed protection will result in a more disturbed and distracted flow, dissipating more of the kinetic energy it poses.

In a sense this highlights one of the flaw of the compiled calculation method: the found velocity at the bed layer u_b is applied in the calculations of scour, under assumption that this velocity at the flow reattachment to the bed location would persist until the end tip of the bed protection where it would then cause scour. In reality some of this velocity would dissipate due to friction losses, depending on the properties of the bed protection. For this reason, slighter scouring would not be surprising.

On the other hand, if the scour development time would truly require 1 or 16 years to reach equilibrium, the North Sea water level rise could counterweight the misaligning velocity values. Sea level rise would increase the hydraulic head difference which is essential for the outflow velocity. This would lead to larger bed layer velocity and scour depth, higher development rate. But it may reduce the open valve durations as Grevelingen would reach its water level limit more rapidly.

At the moment, still a lot of uncertainty remains concerning various pieces in morphological change- scouring assessment. Each piece requires careful assessment in the modelling and design phase, which proves how intricate the topic is.

6. Conclusions and recommendations

Having the results laid out and contemplated on, a comeback to the main research question can be made. The main research question raised and formed the topic of focus for the followed work. Now that the research has been carried out, a light is shone upon the answers it had sought for.

To respond to the question, what kind of morphological bed change would a tidal energy plant implemented in the structure of Brouwersdam lead to, a two-fold answer is required.

As it was already suggested in the section 1.3., a bed morphology will be altered by, firstly, the bed protection securing the toe of the barrier. The results of the sluiceway exit and bed velocity, shear stress calculations and comparison to grain flow resistance are very clearly indicating that bed protection is a necessity for the success of the project. Sand particles are unable to withstand the projected hydraulic conditions downstream of the barrier, therefore an intervention of placing large grain multi-layered bed protection enhancing the flow resistance will be one of the bed morphology changing components. However, this was expected from the beginning. Even if the performed research provided a stronger base and more particular design criteria.

In addition to it, the research indicates the magnitude and scope of bed scouring downstream of the bed protection, that can be expected if the intended energy production system is realized. Section 4.5. shows that morphological change will show a glimpse of it rather quickly, but to develop into a full shape will require a decade long time period. Less figuratively speaking, bed scour will start developing instantly and rapidly in the beginning, slowing down as time passes and gradually reducing in development rate.

Beyond the goal of answering the research question, the research provides an algorithm for the scour assessment, involving evaluation of the key flow properties and flow resistance defining parameters. A thorough literature analysis was conducted in order to comprehend the nature of scouring phenomenon, drawing links between the hydraulic conditions defining parameters and how it relates to scouring. On top of it, a case-specific analysis was conducted to predict the erosive forces behavior around Brouwersdam by applying a freshly developed scour assessment scheme.

Although, it is rather simplistic, operating under a few rational and conservative assumptions, it is still able to project reasonable outcomes for the predefined Climate Power Plant conditions.

Indeed, bed scouring around Brouwersdam is an issue requiring protective and mitigation measures to ensure fortunate execution of the project. The task to minimize the erosive damage can be covered from multiple perspectives. Starting with the main cause of scour-the water flow, investigations should be undertaken to maximize hydraulic head loss at no loss of energy production or to an acceptable amount. This can involve the choice of the turbine, its location within the duct, the geometry of the orifice, through which it enters and exits the sluiceway. Furthermore, a research of the most advantageous bed protection should be undertaken, not only regarding flow resistance and costs, but also its roughness

and flow kinetic energy dissipation capacity. This way, the most calm flow conditions at a lowest possible velocity can be created before the flow reaches the downstream area of the bed protection, where scour is impossible to be prevented. According studies of minimizing scour hole damage to the bed protection are welcome as well, to ensure that the occurring scour would not impinge the integrity and functioning of the bed protection upstream. Scour hole slope reinforcement in the most optimal manner would be complementary. A notion should kept that as long as there is flow, scour will occur anyhow, only its location and severity may vary. As long as the scour takes place where it results in no direct or indirect danger to Brouwersdam structure, it can be allowed. As long as this condition is fulfilled, bed scour assessment duty can be considered complete.

7. References

- Albertson, M. L., Dai, Y. B., Jensen, R. A., Rouse, H. (1948). *Diffusion of Submerged Jets*.
- Arcement, G. J., Schneider, V. R., (1989). *Guide for Selecting Manning's Roughness Coefficients for Natural Channels and Flood Plains*.
- Baarda, B. (2014). *Research. This is it! Guidelines how to design, perform and evaluate quantitative and qualitative research*.
- Batchelor, G. K. (1967). *An Introduction to Fluid Dynamics*.
- Battjes, J. A., Labeur, R. J. (2014). *Open Channel Flow*.
- Berkel, J. van, Maas, J.H., van Schaick, S.J., & Heutink, A. (2018). *Climate Power Plant for Water Safety and Renewable Energy*.
- Bey, A., Faruque, M. A. A., & Balachandar, R. (2007). *Two-Dimensional Scour Hole Problem: Role of Fluid Structures*.
- Biron, P. M., Robson, C., Lapointe, M. F., Gaskin, S. J. (2004). *Comparing different methods of bed shear stress estimates in simple and complex flow fields*.
- Bormann, N. E., Julien, P.Y. (1991). *Scour downstream of grade control structures*.
- Breusers, H. N. C. (1967). *Time scale of two dimensional local scour*.
- Broekema, Y. (2020). *Horizontal shear flows over a streamwise varying bathymetry*.
- Broekema, Y. B., Labeur, R. J., & Uijttewaal, W. S. J. (2019). *Suppression of vertical flow separation over steep slopes in open channels by horizontal flow contraction*.
- Broekema, Y. B., Labeur, R. J., & Uijttewaal, W. S. J. (2018). *Observations and analysis of the horizontal structure of a tidal jet at deep scour holes*.
- Brown, G. O. (2002). *The History of the Darcy-Weisbach Equation for Pipe Flow Resistance*.
- CBS. (2020). *Renewable energy consumption has grown by 16 percent*. Retrieved from <https://www.cbs.nl/en-gb/news/2020/22/renewable-energy-consumption-up-by-16-percent>
- Chatterjee, S. S., Ghosh, S. N., & Chatterjee, M. (1994). *Local scour due to submerged horizontal jet*.
- Chiew, Y. (1992). *Scour Protection at Bridge Piers*.
- Chin, C.O., Li, W. (2002). *Propeller Induced Scour*.
- Crowley, R., Bloomquist D., van de Sande, S. and Lescinski, J. (2020). *Characterization of Bed Stresses near Quay Walls Due to Ship Thruster and Propeller Wash*.
- Doorewaard, P. V. (2010). *Designing a Research Project*.

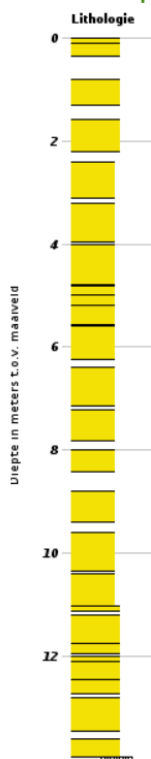
- Engineers Edge, LLC. *Fluid Volumetric Flow Rate Equation*. Engineers Edge. Retrieved 2021-04-19.
- Evans, R. L. (2007). *Fueling our future : an introduction to sustainable energy*.
- Ferro, V. (2003). *Flow resistance in gravel-bed channels with large-scale roughness*.
- Fenton, J. D. (2010). *Calculating resistance to flow in open channels*.
- Firouzia, A., Yang, W., Shi W., & Li C. (2021). *Failure of corrosion affected buried cast iron pipes subject to water hammer*.
- Fourier, J. B. J. (1824). *On the Temperatures of the Terrestrial Sphere and Interplanetary Space*.
- Ghidaoui, M. S., Zhao, M., McInnis, D. A., & Axworthy, D. H. (2005). *A Review of Water Hammer Theory and Practice*. *Applied Mechanics Reviews*.
- Hamill, G. A., Johnston, H. T., & Stewart, D. P. (1999). *Propeller wash scour near quay walls*.
- Hoffmans, G. J. (1998). *Jet scour in equilibrium phase*.
- Hoffmans, G. J. C. M., Booij, R. (1993). *Two-dimensional mathematical modelling of local-scour holes*.
- Hoffmans, G. J. C. M., Pilarczyk, K.W. (1995). *Local scour downstream of hydraulic structures*.
- Hoffmans, G., Verheij, H. (2011). *Jet scour*.
- Hussain, A., Ahmadb, Z., Ojhab, C.S.P. (2016). *Flow through lateral circular orifice under free and submerged flow conditions*.
- Intergovernmental Panel on Climate Change, F. A. (2014). *Climate Change Synthesis Report Summary for Policymakers*.
- Labour, R.J., Uijttewaal, W.S.J. (2019). *Eastern Scheldt storm surge barrier: Linking laboratory experiments to field observations*.
- Luo, M., Wang, X. K., Yan, X. F., Huang, E. (2020). *Applying the mixing layer analogy for flow resistance evaluation in gravel-bed streams*.
- Lysenko, V. P. (1980). *Determination of the coefficient of friction of cohesionless soils on polymer film facings of Earth structures*.
- Maas, J.H., van Schaick, S.J., & van Berkel, J. (2018). *Playing with Currents*.
- Manning, R. (1891). *On the flow of Water in Open Channels and Pipes*.
- Moore, J. R., Komar, P. D. (1991). *CRC Handbook of coastal processes and erosion*.
- Movahedi, A., Kavianpour, M. R., & Yamini, O. A. (2018). *Evaluation and modeling scouring and sedimentation around downstream of large dams*.

- Nielsen, P. (2015). *Basic Coastal Sediment Transport Mechanisms. International Compendium of Coastal Engineering.*
- Rijn, L. C. van (1984). *Sediment Transport, Part III: Bed forms and alluvial roughness.*
- Rijn, L. C. van. *Simple general formulae for sand transport in rivers, estuaries and coastal waters.*
- Rijn, L. C. van (2007). *A Unified view of sediment transport by currents and waves, Part I: Initiation of motion, bed roughness and bed load transport.*
- Roubos, A., Verhagen, H. J. (2007). *Uncertainties in the design of bed protections near quay walls.*
- Saase, M. V. (2018). *The Conceptual Design of a Tidal Power Plant In The Brouwersdam.*
- Schiereck, G. J., Verhagen, H. J. (2012). *Introduction to Bed, Bank and Shore Protection (2nd ed.)* Delft, The Netherlands: VSSD
- Shields, A. (1936). *Application of similarity principles and turbulence research to bed-load movement.*
- Stive, M. J. F., Schipper, M. A., Lujendijk, A. P., Aarninkhof, S. G. J., van Gelder-Maas, C., van Thiel de Vries, J. S.M., de Vries, S., Henriquez, M., Marx, S., Ranasinghe, R. (2013). *A New Alternative to Saving Our Beaches from Sea-Level Rise: The Sand Engine.*
- United Nations (1992). *United Nations Framework Convention on Climate Change.*
- Wal, M. van der, Driel, G. van & Verheij, H. J. (1991). *Scour Manual.*
- Whittaker, J. G., Schleiss, A. (1984). *Scour Related to Energy Dissipaters.*

Appendix

Brouwersdam substrate data. Taken from Dinoloket:

Boormonsterprofiel

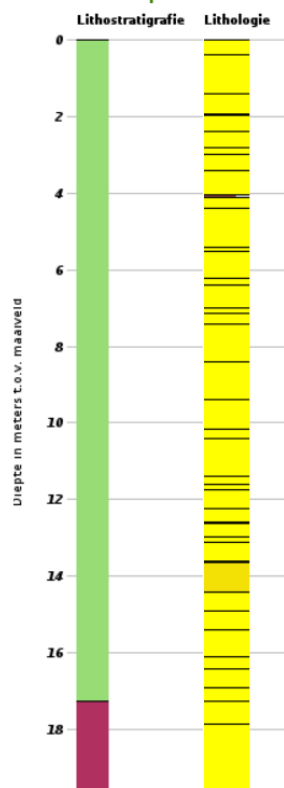


Identificatie : B42F1224
 Coördinaten : 50049 , 421633 (RD)
 Maaiveld: -11.35 m t.o.v. NAP
 Beschikbare informatie: Gescande documenten en Digitale opnamegegevens
 Beschrijfmethode: Onbekend

Lithologie

■ Zand midden categorie
 □ Geen monster

Boormonsterprofiel



Identificatie : B42E0250
 Coördinaten : 49912 , 421474 (RD)
 Maaiveld: -8.60 m t.o.v. NAP
 Beschikbare informatie: Gescande documenten en Digitale opnamegegevens
 Beschrijfmethode: Overig
 Kwaliteit interpretatie: Niet gevalideerd in ondergrondmodel

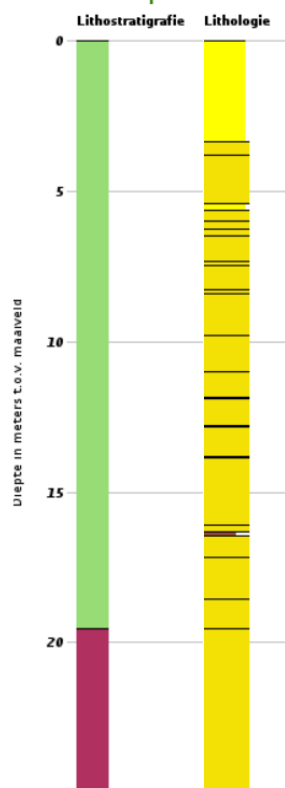
Lithostratigrafie

■ NAWA
 ■ KR

Lithologie

■ Klei
 ■ Zand fijne categorie
 ■ Zand midden categorie
 ■ Veen

Boormonsterprofiel

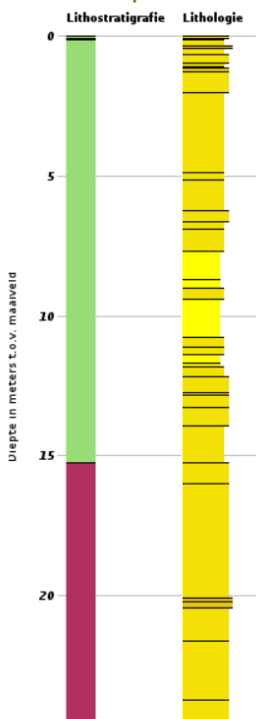


Identificatie : B42E0239
 Coördinaten : 49730 , 421774 (RD)
 Maaiveld: -3.96 m t.o.v. NAP
 Beschikbare informatie: Gescande documenten en Digitale opnamegegevens
 Beschrijfmethode: Overig
 Kwaliteit interpretatie: Niet gevalideerd in ondergrondmodel

Lithostratigrafie **Lithologie**

■ NA	■ Klei
■ KR	■ Zand fijne categorie
	■ Zand midden categorie
	■ Veen

Boormonsterprofiel



Identificatie : B42E0241
 Coördinaten : 49653 , 421589 (RD)
 Maaiveld: -10.12 m t.o.v. NAP
 Beschikbare informatie: Gescande documenten en Digitale opnamegegevens
 Beschrijfmethode: Overig
 Kwaliteit interpretatie: Niet gevalideerd in ondergrondmodel

Lithostratigrafie **Lithologie**

■ NAWA	■ Zand fijne categorie
■ NIHO	■ Zand midden categorie
■ NA	■ Zand grove categorie
■ KR	■ Veen